Using machine learning to detect pedestrian locomotion from sensor-based data

A Thesis Document
Presented to
the Faculty of the College of Computer Studies
De La Salle University Manila

In Partial Fulfillment
of the Requirements for the Degree of
Master of Science in Computer Science

by

NGO, Courtney Anne

Solomon SEE
Adviser
Roberto LEGASPI
Co-Adviser

April 15, 2014

Abstract

The integration of low cost micro-electro-mechanical (MEM) sensors into smart phones have made inertial navigation systems possible for ubiquitous use. Many research studies developed algorithms to detect a user's steps, and to calculate a user's stride to know the position displacement of the user. Subsequent research have already integrated the phone's heading to map out the user's movement across a physical area. These research, however, have not taken into account negative pedestrian locomotion, wherein the user is moving but is not exhibiting any position displacement.

This research aims to solve this problem by collecting positive and negative pedestrian locomotion with data from phone-embedded sensors positioned in the research subject's front pocket. Using these data, a model will be built to classify negative pedestrian locomotion from positive ones.

Keywords: statistical computing model, digital signal processing, inertial navigation systems, MEM sensors, etc.

Table of Contents

List of Figures

List of Tables

1 Research Description

This chapter discusses the current technologies in inertial navigation. This also covers the objectives, scope and limitations of the research, significance of the research, and the research methodology.

1.1 Overview of the Current State of Technology

According to (Shala & Rodriguez, 2011), inertial navigation systems (INSs) determine the path taken by a person based on data gathered from inertial sensors. Inertial sensors that are usually used in these INSs include accelerometers and gyroscopes. Smart phones currently already employ these sensors as micro-electrical-mechanical systems (MEMS) devices, making it possible for INSs to be applied in smart devices and possibly for ubiquitous use.

Unlike other navigation systems, INSs do not continuously calculate for the path with the help of fixed measuring instruments. This distinguishes it among other navigation systems as it does not rely on access points unlike with Wi-fi routers in Wi-fi localization, satellites in the Global Positioning System (GPS), or markers in marker-based navigation. Compared to other navigational systems, INSs are independent of its environment, requiring less cost that otherwise would have incurred with the need of access points. This also implies less environment set-up as access points do not need to be installed for the navigation system to operate. Considering that it is a cheaper and simpler alternative, INS appears to be a more attractive approach to building navigation systems.

Using INSs in real-world situations, however, is limited because its MEMS devices are susceptible to noise and gradual drifts that cause cascading errors. Because of this, most existing inertial navigation systems integrate regular checking with access points with known positions such as satellites and Wi-fi routers to calculate the position of the mobile unit to compensate for these inaccuracies (Martin, Krosche, & Boll, n.d.).

Despite these, researchers continued to look into strategies to work around these limitations and make INS independent of these access points. Studies (Li et al., 2012; Shala & Rodriguez, 2011; Won Kim, Jin Jang, Hwang, & Park, 2004) have been using filters such as Kalman filter to address the issue of sensor drifts by providing estimates to reduce error in noisy data, giving more weight to those with stronger confidence. Apart from filters, other strategies include analyzing the signals to measure the step length, and to validate these steps through step

detection, as evident in (Kothari, Kannan, Glasgwow, & Dias, 2012; Shala & Rodriguez, 2011; Moell & Horntvedt, 2012). Step detection is done in various ways, and past studies have used heuristic models in detection. Most look for peaks and valleys in the accelerometer signals that indicate movement or activity. If these spikes pass a certain threshold, studies such as (Kothari et al., 2012; Libby, 2008) consider them as steps. (Shala & Rodriguez, 2011) and (Moell & Horntvedt, 2012) also take into consideration the time gap between detected steps as one step could emit more than one peak and valley. By doing so, the algorithm would not falsely detect more than one step when only one has been made. Other studies like (Lee & Mase, 2001; S. Y. Cho & Park, 2006; Li et al., 2012) additionally incorporated false-step detecting lags, sling windows, and dynamic time warping (Parnandi et al., 2009?; Li et al., 2012; Thanh, Makihara, Nagahara, Mukaigawa, & Yagi, 2012a).

Although these step detection methods were able to give out promising results, they still limit the user from freely stopping and doing various movements in place. This is because their systems are not designed to detect if a person is truly moving from one position to another, making movements such as walking-in-place mislead their systems. In their experiments, subjects walked on pre-defined paths and were expected to continue and stop only when the experiment is finished. This presents a problem because in real-world situations, users are not bound to walk continuously.

Some studies (Susi et al., 2013; Renaudin et al., 2012) made data-based models to detect motion modes of handheld sensors. Motion modes refer to where the subject is holding the phone. It can be held in a swinging hand while the person is walking, it can also be positioned quite stably as when a person is walking while on the phone, and it can also be transferred from the bag to the subject's hand without the subject actually moving from his physical position. The last class is called "irregular movements", movements that move the phone, but the subject is actually not moving from position. Even though the two studies were able to classify irregular movements with a 94% accuracy, the studies did not elaborate what irregular movements were collected.

This research aims to do a more thorough study on irregular movements. In this research, positive pedestrian locomotion is defined as movements that include moving from one physical position to another on foot. Examples of these are walking, jogging, running, and climbing up and down the stairs. False pedestrian locomotions are movements that do not require moving from a position, such as standing. There are, however, some false pedestrian locomotion movements that can simulate movement from position, and can therefore trick the step detection algorithm into detecting that a genuine step has been taken. These activities include walking-in-place, jogging-in-place, running-in-place, and doing

various exercises in place. For INSs to fully function in real-world applications where users are free to do these negative pedestrian locomotion movements, it is imperative that INSs would be robust enough to handle movements such as these. To not limit user activity when using INSs, there is a need for a model that can detect pedestrian locomotion.

1.2 Research Objectives

1.2.1 General Objective

This research aims to build a model that can detect pedestrian locomotion using data from inertial sensors

1.2.2 Specific Objectives

1. To study different features extracted from data taken with tri-axial accelerometers and gyroscopes that can be used in building the model;
2. To build a corpus of pedestrian locomotion by having research subjects participate in daily activities using inertial measured data;
3. To build a machine learning model that can detect pedestrian locomotion;
4. To evaluate the effect of features and window sizes on the performance of the model; and
5. To assess the effect of the model to an INS and its other modules.

1.3 Scope and Limitations of the Research

This research will concentrate on building a pedestrian locomotion detection model using data gathered from inertial sensors. An application will be developed on the Android platform to collect data, and will run on a Samsung Galaxy SII. Subjects will be requested to conduct experiments that will form the data corpus. The movement they will be performing includes positive pedestrian locomotion such as climbing up and down the stairs, and walking; and negative pedestrian locomotion such as walking- and running-in-place, bending down, turning around in place, and various exercises. These activities will not involve any equipment including treadmills, bicycles, and other objects.

The phone will be placed in the front pocket of the user, and a fixed orientation of the phone will be followed. The subjects would be limited to an age bracket of 20 years old to 49 years old. According to (Thanh, Makihara, Nagahara, Mukaigawa, & Yagi, 2012b), age becomes a factor for subjects under 20 years old, and over 50 years old. The difference comes from the former's stabilizing his gait, and the latter's degradation of physical strength. By limiting research subjects to the age bracket of 20 to 49 years old, the model to be generated can be used by a majority of people.

Unlike age, the same study found that gender is not a significant factor in a subject's gait. For this reason, this research will accept subjects of any gender. This study would collect data from a minimum of 30 subjects, following the example lead by (Anguita, Alessandro, Oneto, Parra, & Reyes-Ortiz, 2012). Most of the experiments will be conducted in Gokongwei and Bro Andrew Gonzalez buildings in DLSU-Manila. Research subjects who are non-DLSU students will perform the data collection in other spaces with a similar topology. The topology are therefore limited to level ground, and stairs.

1.4 Significance of the Research

This research will create a model that will aid existing INSs to be more robust. With the model this research aims to build, future INSs can allow its users to do more natural movement that otherwise would have mislead current algorithms. As these errors cascade during its use, it is imperative that true pedestrian locomotion be detected for proper path mapping to be accomplished. In line with this, the corpus to be built in this research differs from existing corpora. Aside from positive pedestrian locomotion movements that are already present in existing corpus, the corpus of this research will also include movements that are classified as negative pedestrian locomotion.

This research would also be instrumental in propagating the application of INS in everyday activities. The significance of INSs's improvement would permit these systems to perform better than other approaches to navigation systems. As INSs only rely on the data gathered from the inertial sensors, and not on fixed instruments like access points and markers, it is a more environment-independent approach. This characteristic makes INSs appealing as it would entail less cost, and less environment set-up. Some applications that can be created using INSs include guide-map applications that can be used in public places, marketing applications for malls, and even a way to track mentally-handicapped patients around a vicinity.

A specific example of an application where the model can be used is considered in creating a museum guide mobile app. As a user enters the museum, the app can start to track the person's location and continue to keep track correctly even when the user stops to look at the museum pieces. Because the app can also derive the person's location via a starting point, it can act as a map and help the user find a specific museum artifact. Alternatively, it can also estimate which museum piece the user is looking at, and give him more information about the piece.

Furthermore, as users continue to use it, authorities would be able to identify "hot spots", or places that people frequent to. By doing so, they can study why these hot spots exist, and what can be done to improve them.

2 Review of Related Literature

This section discusses methodology, algorithms, features, and limitations of existing research.

2.1 Inertial Navigation Systems

INSs (Li et al., 2012; Shala & Rodriguez, 2011; Moell & Horntvedt, 2012) traditionally follow a sequence of phases to compute where a user has traversed: step detection, step length estimation, heading determination, and mapping. The final output of a INS is the path the system predicted the user roamed, which is usually accompanied with a blueprint map of the physical place. It is important that each phase would operate as accurately as possible as an error in one phase could cascade into the following phases. If errors are continuously accepted by the system, the final output would greatly reflect these errors.

When the user starts walking, the system starts collecting data from the inertial sensors: accelerometer, gyroscope, and orientation (to determine heading). The system starts with the step detection phase, which is responsible in determining whether a step has been taken or not. After it detects a step, it would call on the step length estimator to determine the distance of the step taken. It would also simultaneously call on the heading determiner to calculate for the heading of the phone. The distance and the heading would then be used to map the path of the user. After doing these processes continuously during the duration of the user's walk, the path of the whole walk would finally be generated.

The model this research aims to build would be placed before the step detection phase, as shown in Figure 2.1. If the pedestrian locomotion model detects a negative pedestrian locomotion, the system would just disregard the movement. If it does detect a positive pedestrian locomotion, the step detection phase would start to check if steps have truly been taken.

2.1.1 Step Detection Module

As mentioned before, the step detection module is responsible in determining if the user has taken a step. A conventional method of detection is a peak and valley detection as used in (Lee & Mase, 2001; Won Kim et al., 2004; Kothari et al., 2012; Libby, 2008), where each peak and valley must meet a certain threshold.

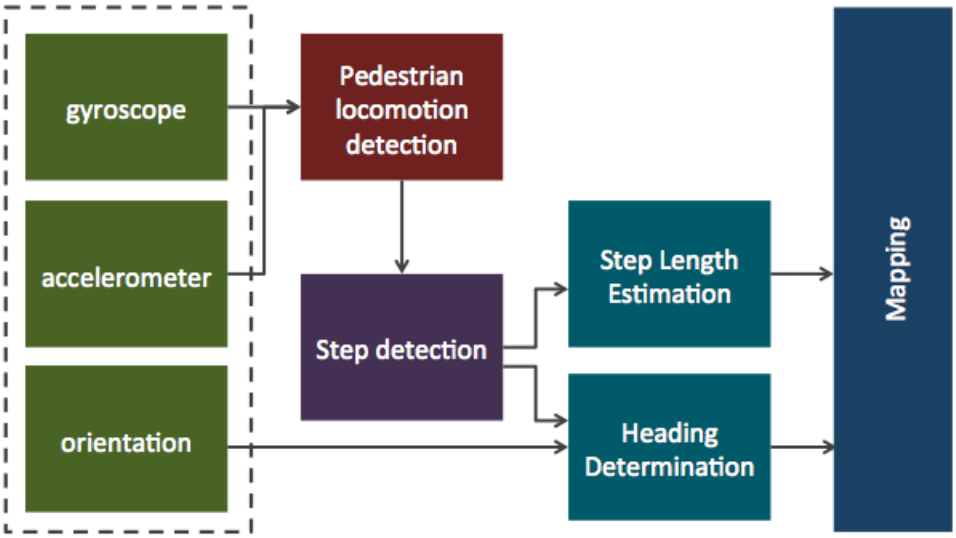

Figure 2.1: Conventional system flow of inertial navigation systems with the model this research aims to create.

In both (Won Kim et al., 2004) and (Lee & Mase, 2001), a pattern of expected vertical and horizontal acceleration when a person takes a step is used in a method called $peak-detectionmethodbasedoncombineddual-axialsignals$ (Ying, Silex, Schnitzer, Leonhardt, & Schiek, 2007). In their research, vertical acceleration corresponds to upward and downward movements, while horizontal accelerations pertain to forward and backward movements. For vertical acceleration, an upper threshold is expected to be reached during the first phase of a step, and another lower threshold at the second phase of the step. For horizontal acceleration, a lower threshold is expected to be achieved the second phase, and a upper threshold at the third phase of the step. Overall, four thresholds should be met at specific time periods of a step.

In (Li et al., 2012), they set two thresholds for changes in the acceleration magnitudes in lieu of peak and valley thresholds. The changes in one step must be more than $1.96m/s^2$, but less than $19.6m/s^2$.

Other step detection algorithms require a minimum time gap in between detected steps. Instead of applying the $peak-detectionmethodbasedoncombineddual-axialsignals$, studies such as (Shala & Rodriguez, 2011) gathered peaks exceeding $12.5m/s^2$ and made sure that only one step can be detected every 350ms. This would discard other peaks of the same step that have also exceeded $12.5m/s^2$. (Lee & Mase, 2001) also implemented a similar heuristic.

2.1.2 Stride Length Estimation Module

The stride length estimation module in an INS calculates the length of a step taken after one is detected. A number of studies (Lee & Mase, 2001; Won Kim et al., 2004; Li et al., 2012) made use of linear models to determine a step length. They have inferred that there exists a linear relationship between step frequency and step length, stating that a user takes bigger steps when walking faster. A frequency model was made in (Li et al., 2012)

(Li et al., 2012) developed a frequency model : $L_g = a * f + b$, where f defined as the walking frequency, and a and b are coefficients that are derived from collected data. In this manner, the coefficients can be altered to make the model specific to a user.

In (Won Kim et al., 2004), they were able to estimate that a step is 60cm long when it takes 0.675 seconds, and 80cm when it takes 0.662 seconds. They also considered the mean of acceleration and they were able to find a relation between it and step length. The mean was found to be around $2.8244 m/s^2$ when a 60cm step is taken, while it is around $5.438 m/s^2$ when taking a 80cm step. They were able to use both step frequency and acceleration mean as heuristics by applying the following equation to determine a stride length:

$$Stride = 0.98 * \sqrt[3]{\sum_{i=1}^{N} \frac{|Acc_{i,mag}|}{N}} \tag{1}$$

where
$Stride$ is the stride length
$Acc_{i,mag}$ is the magnitude of the accelerometer at time i
N is the window size

Aside from step frequency and acceleration mean, variations in acceleration were also taken into account in (S. Y. Cho & Park, 2006; D.-K. Cho, Mun, Lee, Kaiser, & Gerla, 2010; Nam, 2011). Furthermore, they stated that the models were also sensitive to inclination. Because of this, different models were generated for walking on level ground, up slope, and down slope.

2.2 Pedestrian Locomotion Classification

There are currently two studies (Susi et al., 2013; Renaudin et al., 2012) that have created models that consider negative pedestrian locomotion, though there a number of differences from the models and the model this research aims to create. (Susi et al., 2013; Renaudin et al., 2012)'s models considered different orientations which the phone might be held, but also assumed that the phone is generally handheld. Both of these studies classes are as follows:

- Quasi-stable : Subject is showing position displacement, but the phone is exhibiting a quasi-stable position (e.g. texting, phoning, phone is inside the bag)
- Swinging : Subject is showing position displacement, and the phone is also moving, positioned at the subject's swinging hand
- Irregular : Subject is not showing position displacement, but the phone is moving (e.g. subject is taking the phone out of his bag)

In the two studies, negative pedestrian locomotion are categorized under irregular movements. The studies, however, did not elaborate specifically what movements were collected that are considered irregular. Moreover, there is a difference with this study to the two studies as they concentrate on the phones being held in hand.

2.2.1 Corpus

The study (Renaudin et al., 2012) collected data from 12 subjects with an equal number of males and females, and with age ranging from 20-40 years old. The second study (Susi et al., 2013) gathered data from 4 subjects, with 2 men and 2 women.

Data was collected by asking the subjects to walk around a predetermined path that stretches for more than 150m. In the first study, (step length estimation), subjects also had to walk at varying speeds considering slow (0.8 km/h), regular (1.8km/h), and fast (4.0km/h) rates. In both studies, the path to be taken was consistently of the same level, and there was no indicated need that the path must be straight.

The subjects were able to do either of the classes during data collection. In order to keep track of the ground truth, or what the user was actually doing, an

IMU was either placed at the subject's foot or a proctor would administer a wheel sensor to keep track of the user's steps. All of these devices strictly follow GPS time so that synchronization would not cause a problem.

For both studies, an IMU containing a tri-axial gyroscope and a tri-axial accelerometer were used to collect data. Aside from the instances where the phone had to be placed in the bag (under quasi-stable), the IMU was generally handheld. Data from these sensors are collected at a frequency of 100Hz.

2.2.2 Pre-processing

After receiving the signals from the sensors, pre-processing of the sensors would be done before extracting features. Cutting-off outliers would help model generation later on in creating a model. Since it is known that human gait have a frequency of less than 15Hz for both accelerometers and gyroscopes, the data would undergo a Butterworth filter with a 15Hz cut-off.

It is important in these studies to know the orientation of the phone because these IMUs can be held in different ways. This could mean that the accelerometer's x-axis while the IMU is in a bag would not be the same as the accelerometer's x-axis while the IMU is at the hand. In order to treat this problem, the magnitude of each sensor's vector of data would be used instead. To do this, the Euclidean norm of the sensors's vectors would be computed.

$$sens_{i,mag} = \|sens_i\| = \sqrt{(sens_{i,x})^2 + (sens_{i,y})^2 + (sens_{i,z})^2} \tag{2}$$

where
$sens_{i,mag}$ is the magnitude
$sens_{i,x}$ is the x-axis value of the accelerometer/gyroscope at time i
$sens_{i,y}$ is the y-axis value of the accelerometer/gyroscope at time i
$sens_{i,z}$ is the z-axis value of the accelerometer/gyroscope at time i

The magnitude would still contain non-zero DC components, which were also removed afterwards.

A sliding window was then implemented with a 50% overlap. A step was estimated to take 1.28 seconds in the study, as it was not too long or too short for a step. In order to make sure that a step would occur in a span of a window, a sliding of 256 samples was chosen.

2.2.3 Feature Modeling

After pre-processing the raw data, features were extracted to prepare for model generation. The two studies used the same set of features for their classifier: energy, variance, and dominant frequencies. It is notable that these set of features were chosen because it maximizes the differences among inter-class data, and minimized the differences among intra-class data.

The energy was extracted as a feature because it can distinguish a static movement (e.g. standing still) from dynamic movements. The energy can be calculated as follows:

$$energy_i = \frac{1}{N} \sum_{0}^{N-1} {sens_{i,mag}}^2 \tag{3}$$

where
N is the length of the window
$sens_{i,mag}$ is the magnitude of the accelerometer/gyroscope at time i

Variance is also used as feature because it is sensitive to sudden increases which can be indicative of irregular movements.

Dominant frequencies are also used because it is indicative of the position of the IMU on the body. It can be calculated with Short Time Fourier Transform (STFT), a non-computation heavy algorithm. Spectograms shown in the studies exhibited a distinction of dominant frequencies of walking with the IMU (phone swinging in hand), as opposed to having the IMU in hand (talking on the phone). Peaks that are clear in the spectogram reflected the movements when the phone was place at the hand. Additionally, dominant frequencies are distinct from irregular to static to swinging, making it easier for the classifier to predict.

These gives each window a vector of 6 features, 3 features for each sensor.

2.2.4 Data Modelling

All of these features would be used in generating a classifier that can determine whether the phone is at the hand, is assuming a quasi-stable position, or is performing an irregular movement.

Both studies made use of a decision tree to create their models, and the generated model was used before step detection. The model's prediction was crucial in determining what kind of step detection algorithm would be used because there is a different set of heuristics depending on the phone's position.

2.2.5 Results

In the studies, a different set of subjects were asked to participate in evaluating the classifiers. There were also two kinds of evaluation done: controlled tests, and free motion tests. In controlled tests, the subjects had to follow a set of movements that he had to follow strictly. Free-motion tests, on the other hand, also restricts the subject to do a set of activities, but at the subject's choice of sequence.

The accuracies of the model were all high. In (Renaudin et al., 2012), quasi-stable movements were correctly predicted 100% of the time, and swinging was correctly predicted 98% (2% were mispredicted as irregular). In the study, irregular movements was only used as a default value, thus there is no accuracy rate given to this class.

Apart from the swinging and quasi-stable accuracy, the second study (Susi et al., 2013) was able to do free-motion tests, enabling the subjects to do irregular movements. The importance of free-motion tests were stressed as it tests the robustness of the model in a more realistic setting. Still, the model was able to do well. Swinging was predicted correctly 95% of the time, and quasi-stable movements 98% of the time. Irregular movements also reached an accuracy of 98%.

Table 2.1: Confusion matrix of the controlled tests in (Renaudin et al., 2012) and (Susi et al., 2013)

	Texting	Swinging
Texting	100%	0%
Swinging	0%	98% (2% irregular)

Table 2.2: Confusion matrix of the free-motion tests in (Susi et al., 2013)

	Swinging	Texting	Irregular
Swinging	95%	2%	3%
Texting	1%	98%	3%
Irregular	6%	0%	94%

2.3 Modified Step Detection Algorithms

As discussed in Section 1.1 and in Section 2.1.1, some approaches to step detection primarily assumes that the person holding the phone is walking. While their algorithms would be able to catch the instance a person stops walking due to low accelerometer activity, they generally do not take into account when the person is not moving from place but do generate a high accelerometer activity, such as the case in walking-in-place. The following algorithms, on the other hand, have incorporated additional measures that allow their algorithms to recognize if a person is doing the latter kind of activity.

2.3.1 Algorithms

(Thanh et al., 2012a) also had a different method of detecting steps. The research focused on creating a step detection model with data collected from 53 subjects from ages 15-70 years old. The classes are: walking on level-ground, climbing up a flight of stairs, climbing down a flight of stairs, climbing up a slope, and climbing down a slope; their sensors were placed at the waist, at ther person's back. They used support vector machines (SVM) and k Nearest Neighbor (KNN) with Dynamic Time Warping (DTW) as their distance function. According to (Thanh et al., 2012a), DTW calculates the similarity between two signals even if the two signals vary in time or speed. (Thanh et al., 2012a) claimed that by using DTW as their distance function, the speed at which a subject walks is irrelevant as DTW can detect similarities regardless of speed.

In some studies (Lee & Mase, 2001; Li et al., 2012), additional heuristics were implemented to prevent allowing false positive steps.

In (Lee & Mase, 2001), a lag parameter was added in their step detection algorithm. With the lag, the system can supposedly check if the step taken is not a step, but another body movement. It involves getting the z-axis of the accelerometer, which according to (Lee & Mase, 2001) is indicative of upward movements. The lag parameter is as follows:

$$lag = min_{j=0...N}(\sum_{n=0}^{N} z(n)z(n-j)) \tag{4}$$

where
lag is the lag parameter

N is the window length
$z(n)$ is the z-axis value of the accelerometer at time i

The lag must be greater than a threshold to pass the heuristic. As can be seen in the equation, the study assumed that other body movements would have less activity in the accelerometer's z-axis, and that walking would induce peaks in the z-axis.

(Li et al., 2012) further used DTW to detect as an added filter to detect false steps. Aside from (1) checking if peaks and valleys pass a certain threshold, (2) peaks and valleys must also not be too short, or (3) too long (maximum of 1 second). Acceleration's peak and valley's magnitudes are also considered, where (4) the magnitude must be within a minimum of 0.2g, and a maximum of 2.0g.

DTW comes in as a fifth heuristic which acknowledges the similarity of steps taken with the right leg, and similarity of steps taken with the left leg. In this condition, the similarity of the last step taken with the left/right foot and the current step taken with the left/right foot must be greater than a threshold. If the result is negative, a sixth heuristic compares the current left step with the next left step. If these two signal's similarity passes the threshold, the current left step would be considered a step. This heuristic can help in detecting false steps because if a subject stops to walk-in-place, there would be a difference in the signals. But if the subject continues to walk-in-place, there will still be the possibility that "walking-in-place" steps would be considered similar to one another, and thus detected as steps.

2.3.2 Corpus

Building a corpus is not required to create a inertial navigation system, as shown in studies like (Lee & Mase, 2001) where the heuristic model were modeled after studies on gait. Although in other heuristics based models, data were collected to create their heuristic models. In (Li et al., 2012), they collected data from 40 subjects, ending up with a total of 10,000 steps to create their step detection algorithm.

For data-based models, the number of subjects varied from study to study. Some studies collected data only from 4 subjects (Susi et al., 2013), 12 subjects (Renaudin et al., 2012), some with 53 subjects (Thanh et al., 2012a). The biggest inertial-based gait database (Thanh et al., 2012b) had 736 subjects, composed of 382 males and 354 females, with ages ranging from 2 to 78 years old.

For studies like (Li et al., 2012), 50 subjects participated for data collection. The research collected just enough data to build a generic model since personalization would still be needed to make the model work for a specific subject.

2.3.3 Results

In general, adding a heuristic-based or data-based model to detect negative pedestrian locomotion resulted to a more effective system.

The accuracy in (Lee & Mase, 2001) after adding a lag parameter reached an accuracy of 96.3% and 95.8% for detecting level ground and climbing down the stairs respectively. Though the climbing up class only had a 54.2% accuracy, the accuracy went up to 83.3% after using personalized data.

Table 2.3: Performance of the generic model discussed in (Lee & Mase, 2001)

	Level	Up	Down	Missing
Level	96.3%	1.4%	0%	2.3%
Up	38.9%	54.2%	0%	6.9%
Down	2.8%	0%	95.8%	1.4%

Table 2.4: Performance of the personalized model discussed in (Lee & Mase, 2001)

	Level	Up	Down	Missing
Level	96.3%	1.7%	0%	2.0%
Up	11.1%	83.3%	0%	5.6%
Down	0%	2.8%	95.8%	1.4%

In (Li et al., 2012), the number of mispredicted false steps went down from 29 to 14 after adding the data-based model. The model also performed well even when testing the model with freestyle walking (subjects can walk in any style they want) where the mispredicted steps were reduced from 2.51 to 1.22 steps.

In the study, false negatives are more important than false positives. False positives, or the number of mispredicted false steps, can be further checked with the step detection algorithm. Even if a false step was considered a step in the pedestrian locomotion model, there is still the possibility that the false step would be detected as false by the step detection algorithm. The false negatives increased from 0.4 to 0.5. But as stated in the study, the benefits outweighed the disadvantages.

3 Research Methodology

This subsection will describe the research methodology of the study.

3.1 Research Concept Formulation

At this stage, the researcher read on existing studies and explore possible topics that can form the concept of the research.

3.2 Review of Related Literature

A review of previous literature was done to know the current state of research in pedestrian locomotion classification. The researcher began reading studies on digital signal processing to analyze how feature vectors were designed in other studies.

3.2.1 Research Approach

The study followed a quantitative approach. Raw data collected with a smart phone's accelerometer and gyroscope were processed using machine learning algorithms. Data collection, particularly class labelling, was administered by the researcher.

To build the model, it was important to collect a large volume of data that can represent both positive and negative pedestrian locomotion. Therefore a number of test subjects were asked to participate in a set of activities to contribute to the data corpus.

3.3 Data Collection

3.3.1 Data Collection Activities

The activities the test subjects participated on revolve around movements that causes positive and negative pedestrian locomotion. In this research, no instruments apart from the smart phone were used. This means that using equipment such as treadmills was included in the scope of the research.

For the positive pedestrian locomotion, subjects were asked to do each of the following activities for 5 minutes:

- walk
- climb up the stairs
- climb down the stairs

For the negative pedestrian locomotion, subjects were asked to do each of the following activities for 5 minutes:

- stand
- walk-in-place
- leg swings
- turn around
- random movement
- twisting
- bending
- leaning on balls and heels of feet
- sitting

3.3.2 Research Subjects

Based on (Thanh et al., 2012b), age can affect gait recognition for certain age groups. Children under 10 years old and those from ages 10 to 19 had unstable gaits.

Subjects that are members of the "under 10" and "10-19" age brackets affected the gait recognition negatively brought about their unstable gait as these particular subjects are still learning how to walk. Similarly, subjects that are 50 years old and above also have unstable gait due to a degradation in physical strength. The gait recognition, however, was able to perform similarly and well for the rest of the age brackets. For this research, subjects are targeted to be from the age

bracket of 20-49. The subjects can be of any gender, and must be of no physical affliction that may affect his gait.

Following the research done by (Anguita et al., 2012), this research also required 30 subjects for the experiments.

3.3.3 Data Collection Instruments

In order to collect gyroscope and accelerometer readings, a Samsung Galaxy S2 was used as an instrument. The device already has a tri-axial accelerometer and tri-axial gyroscope built inside it. An Android application was developed to collect these readings, and store them for model building afterwards. Only one device was used per experiment.

3.3.4 Data Collection Procedure

Research subjects were asked to participate in the research by doing all of the movement for the indicated time duration. The phone was placed on their front right pocket throughout the length of the activity. The orientation of the phone was placed so that the screen of the phone faced the thigh of the subject, and the top of the phone was pointed to the bottom of the pocket.

The program was set to collect readings at a frequency of 100Hz. According to (Gyllensten & Bonomi, 2011; Ermes, Parkka, Mantyjarvi, & Korhonen, 2008), 20Hz was found to be enough to recognize human gait. With an initial collection of 100Hz at the data collection, future research can lower down the frequency during post-processing depending on the performance of the model generated. Ideally, a lower frequency is better as it would not consume more power as a higher frequency collection would.

During data collection, the program stored three values each from the gyroscope and the accelerometer, corresponding to the three axes.

3.4 Data Pre-processing

Before features can be extracted, the raw data was first pre-processed. A sliding window was implemented with a 50% overlap following the methodology of (Susi et al., 2013; Renaudin et al., 2012). Eight window sizes of lengths 64-, 70-, 80-,

90-, 100-, 128-, 200-, and 256-samples will be used. A program was developed to automatically pre-process the data.

3.5 Feature Extraction

After pre-processing, the features were extracted. During this phase, additional literature was read to learn more about which features can be used for the model.

The list of of features used in the study are listed below. Each window was summarized to a feature vector containing the following features:

- mean of the accelerometer x-axis
- mean of the accelerometer y-axis
- mean of the accelerometer z-axis
- standard deviation of the accelerometer x-axis
- standard deviation of the accelerometer y-axis
- standard deviation of the accelerometer z-axis
- energy of the accelerometer x-axis
- energy of the accelerometer y-axis
- energy of the accelerometer z-axis
- mean of the gyroscope x-axis
- mean of the gyroscope y-axis
- mean of the gyroscope z-axis
- standard deviation of the gyroscope x-axis
- standard deviation of the gyroscope y-axis
- standard deviation of the gyroscope z-axis
- energy of the gyroscope x-axis
- energy of the gyroscope y-axis
- energy of the gyroscope z-axis

- dominant frequency of the accelerometer x-axis
- dominant frequency of the accelerometer y-axis
- dominant frequency of the accelerometer z-axis
- dominant frequency of the accelerometer's Euclidean norm
- dominant frequency of the gyroscope x-axis
- dominant frequency of the gyroscope y-axis
- dominant frequency of the gyroscope z-axis
- dominant frequency of the gyroscope's Euclidean norm

A program was developed by the researcher to automatically extract the time and frequency domain features after pre-processing. One advantage of choosing these features is that they are not computational heavy, making it possible to use the model on-line in future studies.

3.6 Model Generation

The feature vectors were fed to a machine learning algorithm to build the classifier. Following the example of (Susi et al., 2013; Renaudin et al., 2012) and (Li et al., 2012), this research used a decision trees and support vector machines (SVM) to generate the data-based model. WEKA was used to create these models which is capable of running algorithms like C4.5 and SVMs.

Different models using different combinations of features were generated to know which model is the most effective in detecting pedestrian locomotion activities.

The model operated before the step detection module as shown in before in Section 2.1. This approach is distinct from the one taken by the algorithms exposed in Section 2.3. Unlike their proposals where additional measure are incorporated in the step detection module, this research expects the model to operate as a module on its own.

3.7 Data Analysis

In data analysis, the models were tested and their results were analyzed and compared to one another. In this light, the effectivity of the model was assessed. The following are characteristics of the model that were experimented on:

Analyses on the effects of varying window sizes have on the effectivity of the model.

Analysis of the the model algorithm and window sizes on the step detection and stride length estimation module.

A mobile app was developed composed of a step detection module, a stride length estimation module, a heading determination module, and a mapping module. The final result of the app is a map of a user's traversal across a space generated using inertial data. A similar app will be developed with an additional pedestrian locomotion module. A comparison between the two apps allowed this research to observe the effects of adding a pedestrian locomotion model as opposed to having none.

Afterwards, conclusions were made and recommendations were suggested for further research.

3.8 Documentation

The researcher documented the progress and results of the study throughout the duration of the research.

3.9 Calendar of Activities

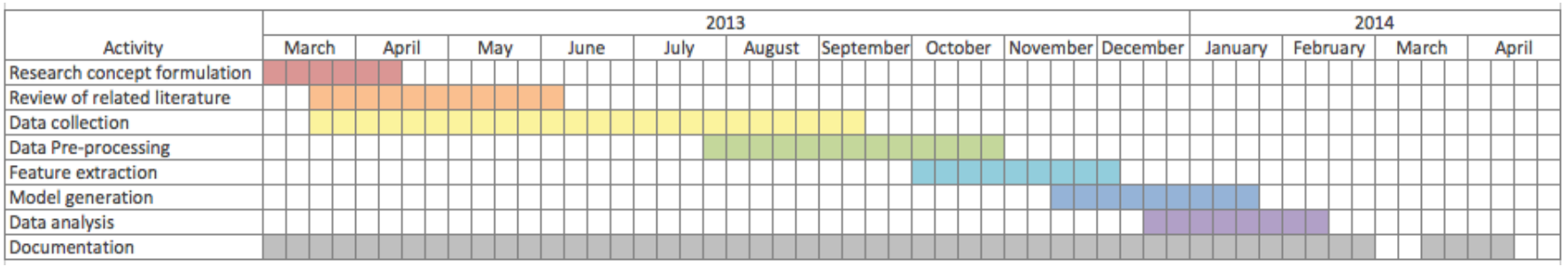

4 Theoretical Framework

This subsection will describe the theoretical framework of the study.

4.1 Sensors

The data gathered from the sensors are already normalized as provided by the phone. The measuring units are dictated in each sensor discussion.

4.1.1 Gyroscope

Gyroscopes are inertial sensors that can measure angular velocity (Aaron Burg, n.d.). Traditional gyroscopes have a mass that spins along an axis independent of the external frame. As the mass vibrates and the external frame is set to place, the mass preserve its initial orientation and will continue to resist changes to its orientation as long as the mass is spinning. These devices are useful in maintaining the balance of a machine such as aircrafts when without any orientation reference (Bryan, n.d.).

Traditional gyroscopes have been in use since the 18th century primarily for marine navigational purposes. The devices soon also proved beneficial in aeronautics exercises by 1916 (Aaron Burg, n.d.). The arrival of silicon machines prompted the entry of micro-electro-mechanical systems (MEMS) technology to create millimeter-size versions of gyroscopes (Aaron Burg, n.d.; *Nanocomputers and swarm intelligence*, 2008). Current commercially-sold smart phones produced contain MEMS gyroscopes that can measure the angular velocity from three axes. In MEMS, the the spinning mass is replaced by a vibrating plate. When the plate is rotated, an output voltage proportional to the angular momentum is triggered (STMicroelectronics, n.d.). MEMS gyroscope typically give its results in radians per second (r/s).

4.1.2 Accelerometer

Accelerometers are devices that measure proper acceleration forces (LLC, n.d.). Accelerometers contain a mass suspended on a spring that interacts with fixed segments of the device. If the accelerometer experiences a positive acceleration in the x-axis, the mass would interact with the respective fixed segment. The

measured displacement of the mass is then given as the acceleration of the x-axis (Android, 2013).

Smart phones currently commercially sold contain a MEMS 3-axis accelerometer. These devices are typically used to know if the phone is in landscape or portrait mode, is being tilted for gaming use, or is experiencing free fall which will trigger the device to cease disk interaction (Inc., 2012). MEMS accelerometers provide the acceleration of the device in meters per seconds square (m/s^2).

4.1.3 Difference between devices

Although all smart phone devices use MEMS sensor chips for their accelerometers and gyroscopes, chips used between devices differ from one another. These chips do not always adhere to the same standard of measuring acceleration and angular velocity, allowing the possibility of conflicting range of values. Aside from using different chips, calibration is also a factor. If two devices are calibrated differently, or are not using the same chip type, a model created over the recorded values of one device are not expected to operate similarly when used in the other device.

Figure 4.1 compares the collected values of a Samsung Galaxy S2 and a CD-R King B1-EP2. The data exhibited are the Euclidean norm of the accelerometer data. Though the difference can turn to be minute when compared to other devices, it can also be as large as shown in the figure. In this example, it is evident that the CD-R King B1-EP2 made use of an accelerometer that responds slower to movement.

One solution to go around the problem of different value ranges across devices is to normalize the values from 0 to 1. Although this tones down the difference between signals, it is still not a prime solution. Figure 4.2 below shows the effect of normalizing the data displayed in the figure before.

4.2 Feature Modelling

This subsection discusses how features will be modelled in preparation for modelling.

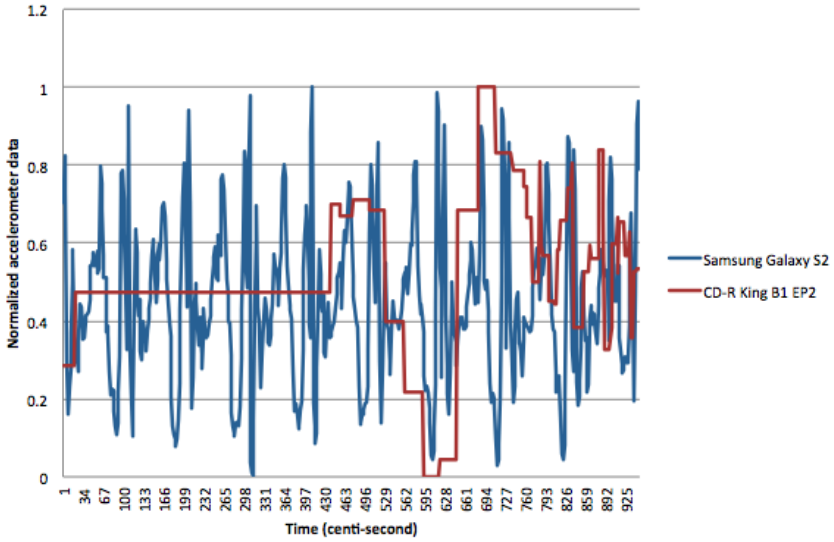

Figure 4.1: Graph showing the difference between values collected by a Samsung Galaxy S2, and a CD-R King B1-EP2, while performing the same movement.

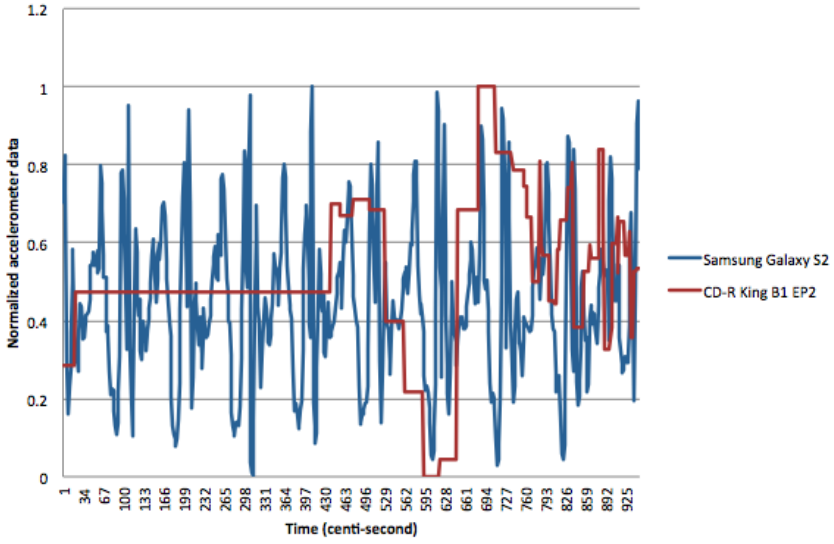

Figure 4.2: Graph showing that normalized values of data collected by two separate phones are still perceptible to variance.

4.2.1 Features

Time domain features that will be extracted from the raw accelerometer and gyroscope data will include a signal window's mean, standard deviation, and signal.

The dominant frequency, a frequency domain feature, will also be extracted from the data. The frequency domain feature will be gathered after the raw signals are processed with short-time Fourier transform (STFT), using the same temporal window used in extracting the time domain features.

Mean The mean of a set of numbers is normally used to estimate where a sample point is "located" when the set is arranged in an ascending order, thus making it a measure of location(Ronald E. Walpole, 2010). Although calculating for the mean has its advantages, it is easily influenced by outliers(Ronald E. Walpole, 2010).

$$Ave_{i,w} = \frac{1}{N}\sum_{i=0}^{N-1} sens_{i,w} \tag{5}$$

where
N is the window size
$Ave_{i,w}$ is the mean of the w-axis of the accelerometer/gyroscope over window i
$sens_{i,w}$ is the w-axis value of the accelerometer/gyroscope at time i
w can either be the x, y, or z-axis

Standard Deviation Getting the variance of a data set aids in understanding the position of a sample point relative to the set's mean(Walpole, 2009). The standard deviation is equivalent to the square root of the variance of a given data set (Ronald E. Walpole, 2010). It is usually used in advantage of its sensitivity to the variance of the upper and lower data samples (Walpole, 2009).

$$Stddev_{i,w} = \sqrt{\frac{1}{N-1}\sum_{i=0}^{N-1}(sens_{i,w} - Ave_{i,w})^2} \tag{6}$$

where
N is the window size
$Stddev_{i,w}$ is the standard deviation of the w-axis over window i
$sens_{i,w}$ is the w-axis value of the accelerometer/gyroscope at time i
w can either be the x, y, or z-axis
$Ave_{i,w}$ is the mean of the w-axis of the accelerometer/gyroscope over window i

Energy The energy of a signal is usually interpreted as the strength of the signal. Given this, a signal's energy can be measured by calculating the area under the curve (Melissa Selik, 2004). To treat the negative samples that accompany digital signals, the square of the signal is computer over a temporal window.

$$Energy_{i,w} = \sum_{i=0}^{N-1} sens_{i,w}^2 \tag{7}$$

where
N is the window size
$Energy_{i,w}$ is the standard deviation of the w-axis over window i
$sens_{i,w}$ is the w-axis value of the accelerometer/gyroscope at time i
w can either be the x, y, or z-axis

The formula used to determine the signal energy is derived from the formula used to identify energy in Physics.(Tan, 2008)

Dominant Frequency The dominant frequency is calculated by getting the frequency with the highest value in the data window. Performing frequency analysis can be beneficial in discriminating two signals. The frequency domain feature has proven to be discriminatory in a research conducted by (Susi et al., 2013). In their research, a dominant frequency was identified when the phone is being swung and a different dominant frequency was found when the phone was being used for texting.

4.2.2 Windowing

Choosing a window size is a vital part in creating a model that deals with signals. In this research, three window sizes will be experimented with. The results shown in Section 4.3 use a window size of 200. The final results will also include experiments with window size of 128, 200, and 256; all three will be treated with a 50% overlap.

Based on an initial trial done calculating the time gaps between steps, the experiment yielded a mean of 0.52 seconds between steps. This would translate to 52 data samples before another step is expected to be taken. The window size is doubled to ensure that at least one step is recorded in each window, which gives 104. Consequently, it would be better to process signals of a length that is an

exponent of 2 in Fourier transform. Given these, 128 is used as it is the nearest number to 104 that is an exponent of 2.

The 200-sample size window is based on the 100Hz sampling rate of the data collection program. This temporal window size will capture a 2-second frame of motion. With reasons akin to the the 128-window size, a window size of 256 is also considered as it is the number that is an exponent of 2 nearest 200.

4.3 Machine learning algorithms

4.3.1 J48

J48 is the WEKA implementation of Quinlan's C4.5 algorithm(Quinlan, 1993). The C4.5 decision tree creates a decision tree based on the attribute values of the available training data. Whenever it encounters a set of items for training, it identifies the attribute with the highest information gain, and designates this attribute as the root node. An attribute is said to have the highest information gain if it is able to discriminate and classify the various instances most clearly. The process is repeated by calculating the information gain of all the other attributes that might branch off from its parent node. This is done until all the data instances are able to follow a path from the root node to a leaf node. There is also the chance that the tree would not be able to accommodate all data instances due to noise.

Using WEKA, a cursory J48 model was created using preliminary data, and a 10-fold cross validation test was done. Even though the data has not yet been completely collected, an accuracy of 87.9% was achieved. Furthermore, a 92.6% recall rate of positive pedestrian locomotion is evident, which is important as the step detection algorithm succeeding the pedestrian locomotion model can further filter out false steps.

4.3.2 SVM

Support Vector Machines (SVMs) is a non-probabilistic binary linear classifier. Given a dataset, the SVM algorithm charts the values into a higher-dimensional space. Using the input data instances or the support vectors as representation, the algorithm would proceed to find the optimal hyperplane separating the different instances of the classes. An optimal hyperplane is similar to linear regression in that it maximizes the gap among the classes. Setting its kernel to a higher exponent would allow the hyperplane be more flexible to the data its trying to

separate. In this paper, a linear function would be used.

An important aspect of SVMs is to find the maximum-margin hyperplane, and this entails solving for the optimum distance of it and the data inputs. Due to the complexity of the optimization algorithms, the learning takes longer and usually requires external quadratic programming solvers. John Platt at Microsoft Research came up with an algorithm that solves this problem in 1998. His algorithm is called sequential minimal optimization (SMO) (Platt, 1999), which strategically cuts down the optimization problem into smaller 2-dimensional sub-problems, and the subproblems are solved analytically. The SMO chooses two Lagrange multipliers iteratively and optimizes the pair. One of these multipliers should violate the Karush-Kuhn-Tucker (KKT) conditions, conditions of which are necessary for non-linear programming to be optimal. Convergence is ensured with SMOs.

As with J48, a preliminary SMO model was also created using the the collected data so far. A 10-fold cross validation test resulted to a 84.4% accuracy. There is also a high recall of positive pedestrian locomotion cases, reaching 91.7%, rendering both J48 and SMO find algorithms to create a sufficient pedestrian locomotion model.

4.4 Inertial Navigation System Modules

4.4.1 Step Detection Module

The step detection module would detect steps from accelerometer signals once the pedestrian locomotion model determines that the user is moving from one place to another.

The accelerometer signals would be scoured for a value greater than threshold α. As shown in Figure 4.4, a lot of values would surpass the set threshold. In order to discard false peaks, a second threshold β is introduced. Threshold β is the minimum time gap between two steps. Before a step is identified, the time gap between the said step and the previous step must be greater than threshold β. In Figure 4.6, the green arrow represents a step whose time difference from its predecessor is being assessed. The initial step would be relieved of satisfying threshold β as it does not have a previous step to refer to. The step detection process is shown in Figures 4.3 to 4.6.

These two thresholds will be determined after collecting data.

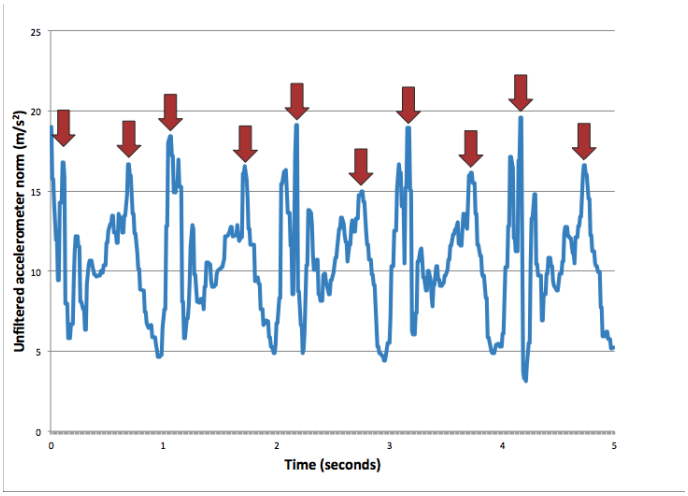

Figure 4.3: Peak generated by steps are indicated by red arrows.

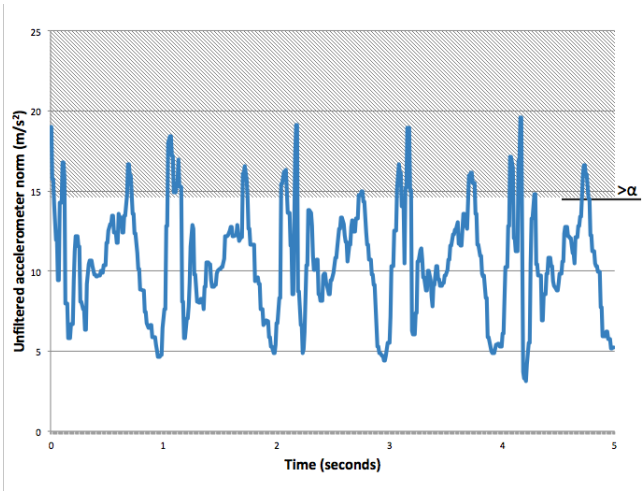

Figure 4.4: The shaded area in the chart shown the data points that have pass threshold α.

4.4.2 Stride Length Estimation Module

The stride length estimation module would start calculating for the step length once the Step Detection Module has determined the user made a step. A linear model would be created as studies have shown before that a linear relationship exists between stride length and step frequency. This module would update the step frequency along with the Step Detection Module. A linear model would be generated after collecting data.

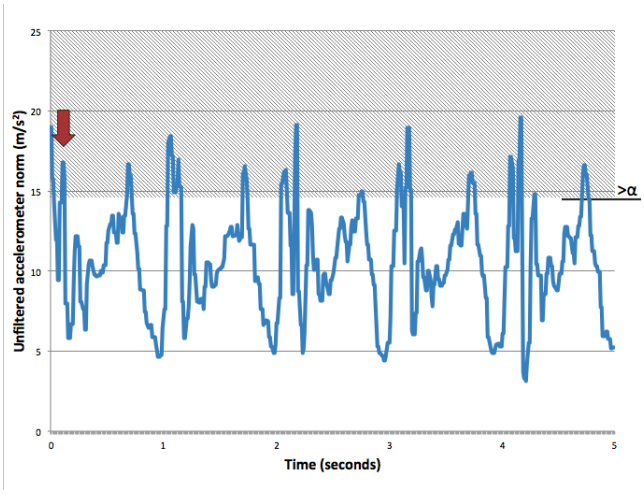

Figure 4.5: The initial step only needs to pass threshold α as there is no previous point to refer to for threshold β.

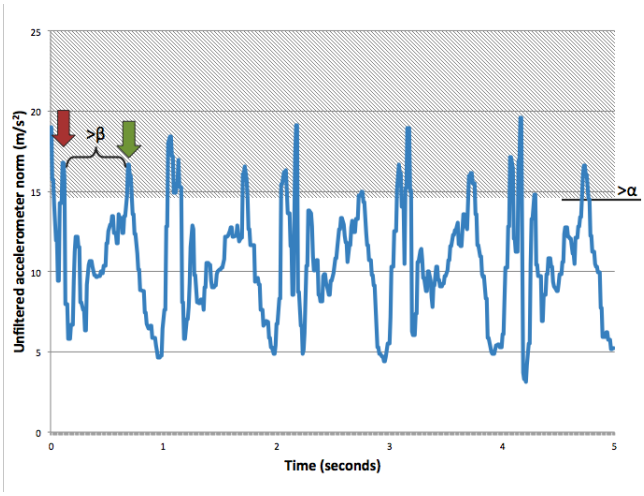

Figure 4.6: Proceeding steps need to have a time gap greater than threshold β between itself and the previous step.

4.4.3 Heading Determination Module

This module would work side-by-side with the Stride Length Estimation Module after the Step Detection Module determines a step has been taken. It is responsible of approximating the direction the user is heading. In this research, the orientation y-axis data would be used to determine the heading. The values can range between 0° to 359°.

4.4.4 Mapping Module

The mapping module outputs a series of points indicating a user's traversal across a space. It would receive inputs from the stride length estimator module and heading determination module, and would have knowledge of the coordinates of the previous point. The coordinates of the initial point would be set to (0,0).

The new point would be calculated as:

$$x_{cur} = l * cos(a) + x_{prev} \tag{8}$$

$$y_{cur} = l * sin(a) + y_{prev} \tag{9}$$

where
x_{cur} is the x-coordinate of the current point
y_{cur} is the y-coordinate of the current point
x_{prev} is the x-coordinate of the previous point
y_{prev} is the y-coordinate of the previous point
l is the stride length
a is the heading

The final predicted path would be relative to the user's initial position, and would be superimposed manually over an actual map of the venue. An actual map would not be used to determine the path of the user.

5 Design issues

5.1 Pedestrian Locomotion Features

Tests were performed to gauge the efficacy of each feature. In the following sections, preliminary data collected in this research were used for the graphs. Each feature was gathered over a window of 200 samples with a 50% overlap.

5.1.1 Mean

The means of the unfiltered Euclidean norm of the accelerometer data were collected as shown in Figure 5.1. The results show that there is a distinction between the means collected when a subject is walking as opposed to when a subject is standing and walking-in-place. Based on the figure, the signals tend to reach higher frequencies when performing positive pedestrian locomotion movements. As compared to the subsequent features, the mean is less distinguishing of positive and negative pedestrian locomotion movements.

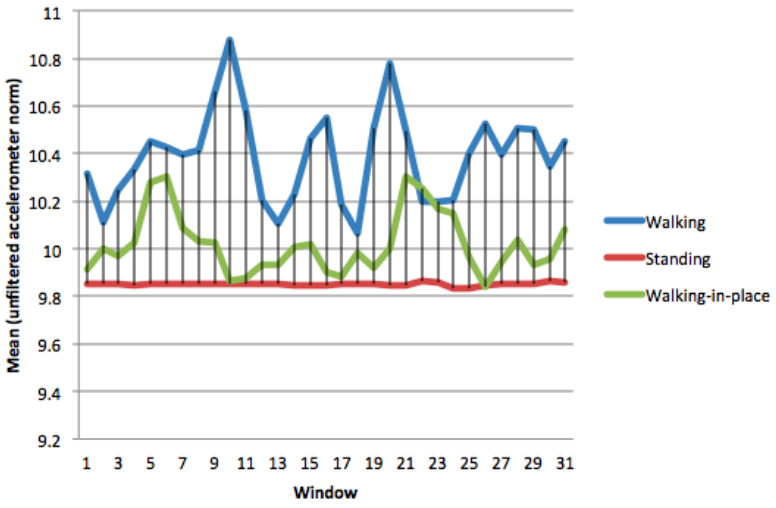

Figure 5.1: Graph showing that means collected while walking are distinct from the means collected when standing or walking-in-place.

5.1.2 Standard Deviation

The standard deviations collected from the preliminary data shows a wide distinction between positive and negative pedestrian locomotion. Using the same data in gathering the means, the standard deviations of the unfiltered Euclidean norm of the accelerometer data were computed. As seen in Figure 5.2, the signals tend to fluctuate more when walking, as opposed to standing. The difference in walking and walking-in-place is explained by a higher y-axis activity when doing the former.

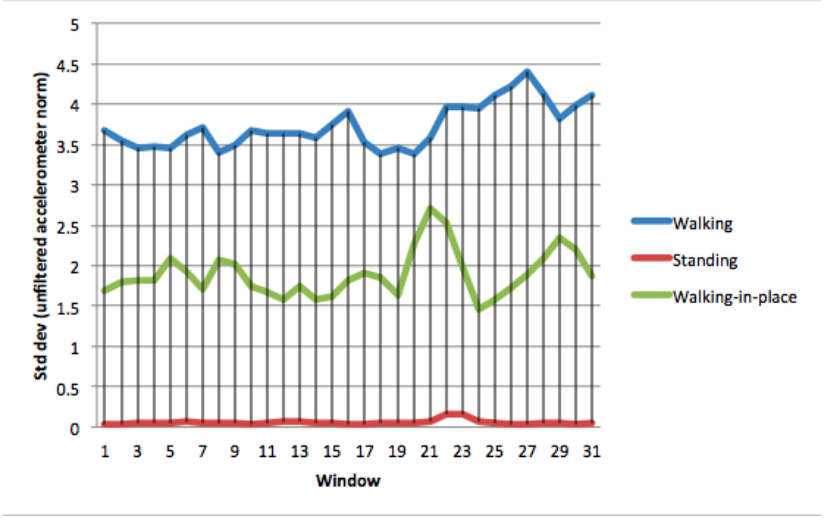

Figure 5.2: Graph showing that the standard deviations collected while walking are distinct from the means collected when standing or walking-in-place.

5.1.3 Energy

Based on the same data set, the energies of the unfiltered Euclidean norm of the accelerometer data were calculated using the same window size. A distinction between walking and standing or walking-in-place can be clearly seen in Figure 5.3, similar to the results displayed by the previous two features. It is evident in this experiment that positive pedestrian locomotion movements contain more energy as opposed to its negative counterpart.

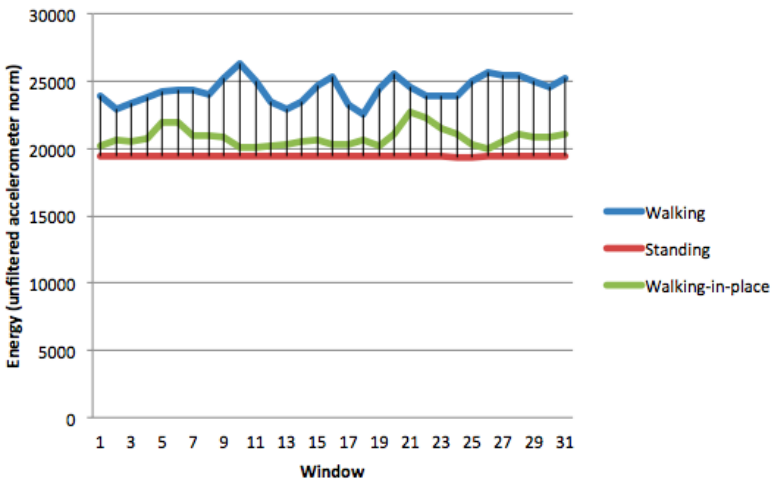

Figure 5.3: Graph showing that energies collected while walking are distinct from the means collected when standing or walking-in-place.

5.1.4 Dominant Frequency

The dominant frequencies were gathered after performing STFT on preliminary data. As can be seen in Figure 5.4, there are parts where the three activities have the same dominant frequency while there are other sections that shows a distinction between the three activities.

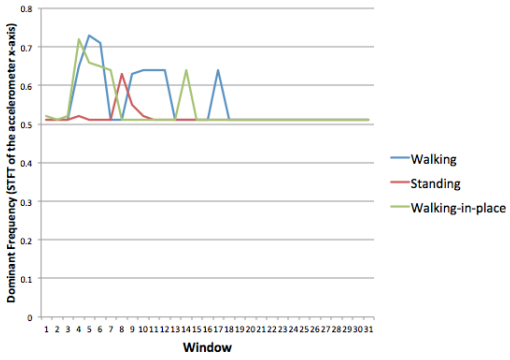

Figure 5.4: Graph showing the dominant frequencies collected from data of subjects walking, standing, and walking-in-place.

5.1.5 Classification Model Performance

Before the data was processed to create models, the data was first balanced to have an equal number of positive and negative instances. A total of eight classification models were then generated with WEKA, four of which are J48 models with varying window sizes, and the rest are the SMO models with four different window sizes. Table 5.1 shows the accuracy evaluated with 10-fold cross-validation. All of the models performed well, and the J48 models performed better over-all than the SMO models.

Table 5.1: Evaluation of J48 and SMO models across different window sizes using 10-fold cross-validation

Window Size - Overlap Size	Algorithm	Accuracy	Recall (Positive pedestrian locomotion)
100-50	J48	94.1%	94.6%
	SMO	89.6%	88.3%
128-64	J48	95.3%	95.9%
	SMO	91.5%	90.1%
200-100	J48	96.4%	96.7%
	SMO	92.3%	91.1%
256-128	J48	97.0%	97.3%
	SMO	93.2%	92.2%

Table 5.1 also presents each model's satisfactory recall on positive pedestrian locomotion activities. It is important that the models achieve a high recall on positive pedestrian locomotion activities because positive movements that are mistaken as negative would lead the INS to discount real steps as false movement. This error would cascade to the estimated number of steps and estimated length traversed by the subject.

6 Results and Analysis

This chapter shows the results and analysis of the tests in the research.

6.1 Tests

This section discusses the tests carried out in this research. Six subjects performed four different tests, and each test is explained in detail below. In collecting these test data, the subjects were limited to follow a marked route, to execute positive and negative pedestrian locomotion activities directed to them, and to only bring out the phone at the beginning and end of each test. The subjects were allowed to walk on their own natural regular pace.

6.1.1 Straight Route

The straight route test is a straight 10 meter walk. Since this test is a purely positive pedestrian locomotion activity, it is imperative that the INS with the prediction module to correctly identify most movements as positive. If not, the conventional INS will show a clear advantage. A visual representation is shown in Figure 6.1.

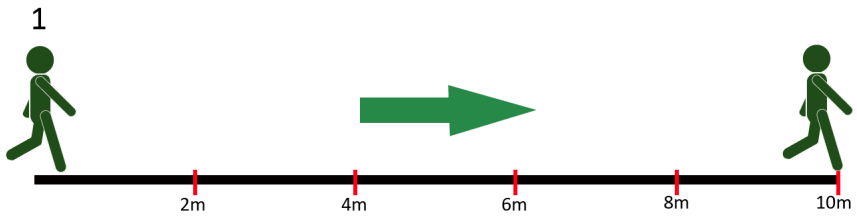

Figure 6.1: The straight route is composed of 1) walking.

6.1.2 Multi-Activity Straight Route

The multi-activity straight route is a straight 10 meter walk with various negative pedestrian locomotion activities done every 2 meters. The routine, which is shown in Figure 6.2, starts with 1) a two meter walk, 2) five seconds of standing, 3) two meter walk, 4) five seconds of walking-in-place, 5) two meter walk, 6) five seconds

of bending, 7) two meter walk, 8) five seconds of leaning on the balls and heels of feet, 9) two meter walk, and 10) five seconds of twisting. Since walking for two meters typically takes less than three seconds, negative instances outnumber the positives. With this, INSs with a prediction model are expected to outperform the INSs without one.

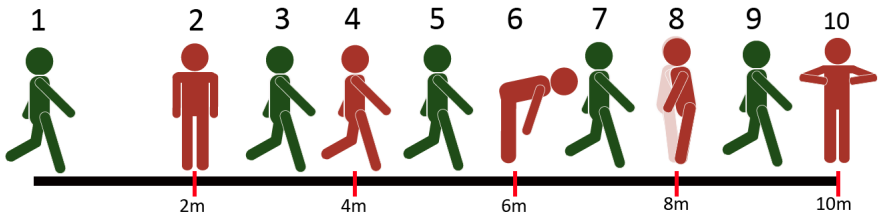

Figure 6.2: The multi-activity straight route is composed of 1) a two meter walk, 2) five seconds of standing, 3) two meter walk, 4) five seconds of walking-in-place, 5) two meter walk, 6) five seconds of bending, 7) two meter walk, 8) five seconds of leaning on the balls and heels of feet, 9) two meter walk, and 10) five seconds of twisting.

6.1.3 Square Route

The square route is a 20 meter walk that is composed of four five-meter sections that are orthogonal after one another. The routine is similar to the straight route in that it is purely a positive pedestrian locomotion activity. This test will not only challenge the INS in correctly identifying changes in orientation, but will also evaluate whether the prediction module can correctly classify "walking while turning" from "turning in place".

6.1.4 Multi-Activity Square Route

A variance of the square route, the multi-activity square route is also a 20 meter walk but with four five-second activities done every five meters. The routine, which is presented in Figure 6.4, begins with 1) a five meter walk, 2) five seconds of standing, 3) five meter walk after a perpendicular turn, 4) five seconds of walking-in-place, 5) five meter walk after a perpendicular turn, 6) five seconds of bending, 7) five meter walk after a perpendicular turn, and 8) five second of twisting. Since walking five meters usually take 3.5 to 5 seconds, this test is the most balanced in terms of number of the positive and negative pedestrian locomotion movements.

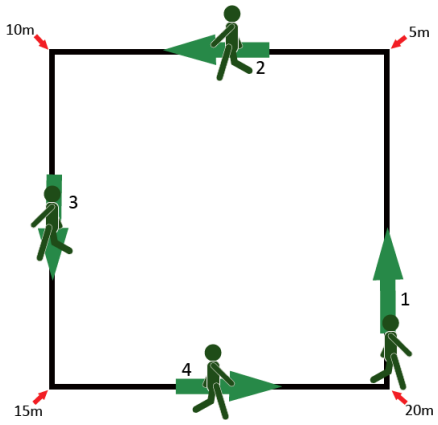

Figure 6.3: The square route is composed of walking and turning at a 90° angle every five meters.

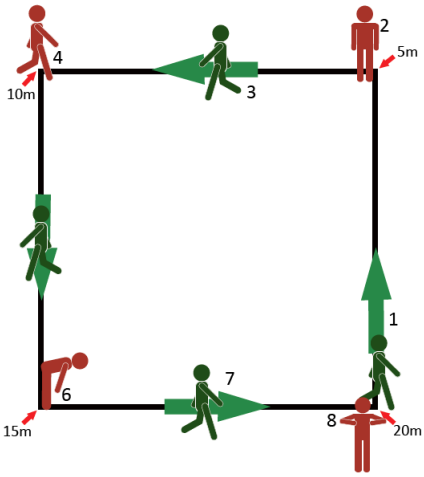

Figure 6.4: The multi-activity square route is composed of 1) a five meter walk, 2) five seconds of standing, 3) five meter walk, 4) five seconds of walking-in-place, 5) five meter walk, 6) five seconds of bending, 7) five meter walk, and 8) five second of twisting.

6.2 Evaluation of the Classification Models

6.2.1 Straight Route

Table 6.1 shows the results of the different models in predicting the data from the straight route test. Since the straight route test is composed of only positive

pedestrian locomotion movements, the INS without a prediction model performed perfectly with an accuracy and recall of 100%. In this test, the accuracy is equivalent to the recall in positive pedestrian locomotion activities because all the movements are positive.

Table 6.1: Accuracy of models predicting the data from the straight route tests. In this test, the accuracy and recall of positive pedestrian locomotion are the same because the test is purely a positive pedestrian locomotion activity.

Window Size - Overlap Size	Model Type	Recall on Walking	Accuracy
64-32	J48	83.15%	83.15%
	SMO	67.42%	67.42%
70-35	J48	62.96%	62.96%
	SMO	17.28%	17.28%
80-40	J48	72.86%	72.86%
	SMO	17.14%	17.14%
90-45	J48	73.77%	73.77%
	SMO	73.77%	73.77%
100-50	J48	88.89%	88.89%
	SMO	87.04%	87.04%
128-64	J48	85.00%	85.00%
	SMO	10.00%	10.00%
200-100	J48	68.18%	68.18%
	SMO	13.64%	13.64%
256-128	J48	62.50%	62.50%
	SMO	18.75%	18.75%

It was observed that the accuracy diminished as the window size increased. This fact was even more accentuated by the decrease of data windows to predict. For example, one subject has ten data windows to be predicted with the 100 sample window. This number was reduced to four with the 256 sample window. This risks a bigger percentage of failure for every misclassification. This effect is present in subsequent tests as well.

In this test, the J48 model with a window size of 100 performed the best of all the models. When each subject was analyzed, three out of six subjects had a 100% accuracy in prediction, while two subjects had one misclassified step each, and the other pulled down the over-all accuracy with four misclassifications. The SMO model with the 100 sample window also had the same predicament. The first five subjects have similar results, but the last subject had five mispredicted steps instead of four.

Table 6.2: Accuracy of models generated with selected attributes predicting the data from the straight route tests. In this test, the accuracy and recall of positive pedestrian locomotion are the same because the test is purely a positive pedestrian locomotion activity.

Window Size - Overlap Size	Model Type	Recall on Walking	Accuracy
64-32	J48	93.26%	93.26%
	SMO	93.26%	93.26%
70-35	J48	87.65%	87.65%
	SMO	27.16%	27.16%
80-40	J48	81.43%	81.43%
	SMO	34.29%	34.29%
90-45	J48	88.52%	88.52%
	SMO	19.67%	19.67%
100-50	J48	92.59%	92.59%
	SMO	77.78%	77.78%
128-64	J48	90.00%	90.00%
	SMO	57.50%	57.50%
200-100	J48	86.36%	86.36%
	SMO	9.09%	9.09%
256-128	J48	87.50%	87.50%
	SMO	37.50%	37.50%

Another set of models, shown in Table 6.2, was also generated that use selected attributes based on their discriminating ability. This set shows that the J48 and SMO models with the 64-sample window size outperformed the models with the 100-sample window size. Compared to the previous set of models, the models that only used selected attributes achieved higher accuracies.

6.2.2 Multi-Activity Straight Route

The results for the multi-activity straight route test is shown in Table 6.3. The accuracy of the INS without a model was also included in the results to show the advantage of using a model. In these test, the highest accuracy was achieved by the J48 model using 100 sample window with 77.93%. This was closely followed by the SMO model of the same window size with 76.58%.

Though this tests show the benefits of using a prediction model, the models performed less competently compared to those in the straight route test. One possible reason is the way the subjects reacted to the markers, especially with

Table 6.3: Performance of models predicting the data from the multi-activity straight route tests.

Window Size - Overlap Size	Model Type	Recall on Walking	Recall on Not Walking	Accuracy
64-32	without	100.00%	0.00%	30.95%
	J48	67.59%	76.76%	73.93%
	SMO	63.89%	42.74%	49.28%
70-35	without	100.00%	0.00%	33.23%
	J48	57.55%	79.34%	72.10%
	SMO	5.66%	90.14%	62.07%
80-40	without	100.00%	0.00%	31.65%
	J48	57.95%	74.21%	69.06%
	SMO	6.82%	92.63%	65.47%
90-45	without	100.00%	0.00%	31.71%
	J48	56.41%	76.79%	70.33%
	SMO	56.41%	76.79%	70.33%
100-50	without	100.00%	0.00%	32.43%
	J48	73.61%	78.67%	77.03%
	SMO	83.33%	72.67%	76.13%
128-64	without	100.00%	0.00%	34.12%
	J48	67.24%	78.57%	74.71%
	SMO	3.45%	83.93%	56.47%
200-100	without	100.00%	0.00%	35.51%
	J48	52.63%	76.81%	68.22%
	SMO	2.63%	91.30%	59.81%
256-128	without	100.00%	0.00%	34.57%
	J48	28.57%	83.02%	64.20%
	SMO	3.57%	88.68%	59.26%

this particular test. Because of the short two meter distance given, the subjects shorten their strides to fit the two meter distance, which the model may have had a hard time trying to classify.

There is also a decline in the models's accuracy as it went from a window of 100 to a window of 128. The performance also deteriorated to the next two bigger window sizes. The increase of transitions is one cause to this. With the 100 sample window, there are data windows that are the transitions from a negative pedestrian locomotion to a positive, or vice versa. For example, one transition window is 60% walking and the other 40% is standing. As the window size grew, the transition windows gained more weight with the decrease of windows, and the misclassification of these transitions also increased. For this test, the J48 model

only had 8 misclassifications of transitions with the 100 sample window. This grew to 13 in the 128 sample window, 17 for the 200 sample window, and 22 to the last window size. The same issue also arose for the SMO models. Though there were still a number of non-transition seconds that were misclassified, the addition of the transitions could have been avoided with a smaller window size. This effect also exists in the other tests.

Table 6.4: Performance of models generated with selected attributes predicting the data from the multi-activity straight route tests.

Window Size - Overlap Size	Model Type	Recall on Walking	Recall on Not Walking	Accuracy
64-32	without	100.00%	0.00%	30.95%
	J48	80.56%	65.56%	70.20%
	SMO	91.67%	21.58%	43.27%
70-35	without	100.00%	0.00%	33.23%
	J48	78.30%	73.24%	74.92%
	SMO	12.26%	95.31%	67.71%
80-40	without	100.00%	0.00%	31.65%
	J48	67.05%	74.74%	72.30%
	SMO	7.95%	95.26%	67.63%
90-45	without	100.00%	0.00%	31.71%
	J48	76.92%	69.05%	71.54%
	SMO	5.13%	97.02%	67.89%
100-50	without	100.00%	0.00%	32.43%
	J48	84.72%	68.67%	73.87%
	SMO	68.06%	66.00%	66.67%
128-64	without	100.00%	0.00%	34.12%
	J48	84.48%	70.54%	75.29%
	SMO	22.41%	93.75%	69.41%
200-100	without	100.00%	0.00%	35.51%
	J48	86.84%	65.22%	72.90%
	SMO	2.63%	98.55%	64.49%
256-128	without	100.00%	0.00%	34.57%
	J48	78.57%	60.38%	66.67%
	SMO	3.57%	94.34%	62.96%

Another set of models built with selected attributes were also generated and evaluated. As can be seen in its results in Table 6.4, this set achieved slightly poorer results compared to its former counterpart.

6.2.3 Square Route

The results of the prediction models's classification of data from the square route tests are presented in the Table 6.5. Similar to the straight route tests, the INS without a prediction module correctly classified all movements as positive, and has a 100% accuracy.

Table 6.5: Accuracy of models predicting the data from the square route tests. In this test, the accuracy and recall of positive pedestrian locomotion are the same because the test is purely a positive pedestrian locomotion activity.

Window Size - Overlap Size	Model Type	Recall on Walking	Accuracy
64-32	J48 SMO	82.21% 76.69%	82.21% 76.69%
70-35	J48 SMO	74.00% 26.67%	74.00% 26.67%
80-40	J48 SMO	85.27% 25.58%	85.27% 25.58%
90-45	J48 SMO	79.82% 79.82%	79.82% 79.82%
100-50	J48 SMO	97.03% 99.01%	97.03% 99.01%
128-64	J48 SMO	93.51% 6.49%	93.51% 6.49%
200-100	J48 SMO	71.11% 4.44%	71.11% 4.44%
256-128	J48 SMO	82.35% 2.94%	82.35% 2.94%

As with the straight route test, the J48 and SMO models with the 100 sample window size outperformed the other window sizes with 96.97% and 98.97% accuracy each. Upon analyzing the performance of the J48 model per subject, three subjects had data that were all correctly classified while the other three had one misclassification each. The SMO model correctly classified all instances as positive except for one misprediction.

The results of the set of models generated using selected attributes are shown in Table 6.6. Similar to what is shown in the Straight Route tests, the models created with selected attributes fared better in purely positive test cases. Though there are only a few instances where the J48 models in the new set performed more exceptionally that the original set of models, the SMO models generally performed better with the selected attributes.

Table 6.6: Accuracy of models generated with selected attributes predicting the data from the square route tests.

Window Size - Overlap Size	Model Type	Recall on Walking	Accuracy
64-32	J48	96.93%	96.93%
	SMO	98.16%	98.16%
70-35	J48	98.00%	98.00%
	SMO	39.33%	39.33%
80-40	J48	91.47%	91.47%
	SMO	38.76%	38.76%
90-45	J48	95.61%	95.61%
	SMO	31.58%	31.58%
100-50	J48	99.01%	99.01%
	SMO	89.11%	89.11%
128-64	J48	94.81%	94.81%
	SMO	63.64%	63.64%
200-100	J48	97.78%	97.78%
	SMO	33.33%	33.33%
256-128	J48	97.06%	97.06%
	SMO	52.94%	52.94%

6.2.4 Multi-Activity Square Route

Table 6.7 shows the result of the models in predicting the data from the multi-activity square route tests.

The multi-activity square route test is a good way to evaluate the models's ability to predict because of the balanced number of positive and negative pedestrian locomotion activities. As the results in Table 6.7 show, the J48 and SMO model with the 100 sample window outperformed the rest of the models. The two models, especially the SMO model, achieved a good recall on positive pedestrian locomotion activities with 92.98%. Though their recall on negative pedestrian locomotion movements are lower, the recall on positive instances are more important.

The results of the models generated using selected attributes are presented in Table 6.8. The performance of the original J48 models and the ones using the selected attributes are close, but the SMO models have higher accuracies with the selected attributes. In this test, the highest performing model is the J48 model with the 128-sample window size with a 82.51% accuracy.

Table 6.7: Performance of models predicting the data from the multi-activity multi-activity square route tests.

Window Size - Overlap Size	Model Type	Recall on Walking	Recall on Not Walking	Accuracy
64-32	without	100.00%	0.00%	48.66%
	J48	76.80%	70.68%	73.66%
	SMO	73.48%	42.93%	57.80%
70-35	without	100.00%	0.00%	48.67%
	J48	72.73%	70.11%	71.39%
	SMO	20.61%	87.36%	54.87%
80-40	without	100.00%	0.00%	48.65%
	J48	80.56%	73.68%	77.03%
	SMO	12.50%	93.42%	54.05%
90-45	without	100.00%	0.00%	49.62%
	J48	80.00%	77.27%	78.63%
	SMO	80.00%	77.27%	78.63%
100-50	without	100.00%	0.00%	48.51%
	J48	87.72%	67.77%	77.45%
	SMO	90.35%	71.07%	80.43%
128-64	without	100.00%	0.00%	48.09%
	J48	87.50%	68.42%	77.60%
	SMO	7.95%	85.26%	48.09%
200-100	without	100.00%	0.00%	51.75%
	J48	72.88%	60.00%	66.67%
	SMO	6.78%	92.73%	48.25%
256-128	without	100.00%	0.00%	51.14%
	J48	84.44%	67.44%	76.14%
	SMO	8.89%	90.70%	48.86%

6.3 INS Performance

This section discusses the effect of the prediction module on the step detection module, stride length estimation module, and mapping module. The following results use models generated with a 100 sample window using all attributes as this window size generated the best performing models as shown in Figure C.1.

Table 6.8: Performance of models generated with selected attributes predicting the data from the multi-activity square route tests.

Window Size - Overlap Size	Model Type	Recall on Walking	Recall on Not Walking	Accuracy
64-32	without	100.00%	0.00%	48.66%
	J48	85.64%	61.78%	73.39%
	SMO	96.13%	21.99%	58.06%
70-35	without	100.00%	0.00%	48.67%
	J48	86.06%	68.39%	76.99%
	SMO	23.03%	84.48%	54.57%
80-40	without	100.00%	0.00%	48.65%
	J48	89.58%	63.82%	76.35%
	SMO	28.47%	82.89%	56.42%
90-45	without	100.00%	0.00%	49.62%
	J48	89.23%	70.45%	79.77%
	SMO	20.77%	90.15%	55.73%
100-50	without	100.00%	0.00%	48.51%
	J48	90.35%	60.33%	74.89%
	SMO	80.70%	71.07%	75.74%
128-64	without	100.00%	0.00%	48.09%
	J48	94.32%	71.58%	82.51%
	SMO	59.09%	90.53%	75.41%
200-100	without	100.00%	0.00%	51.75%
	J48	93.22%	60.00%	77.19%
	SMO	16.95%	78.18%	46.49%
256-128	without	100.00%	0.00%	51.14%
	J48	88.89%	67.44%	78.41%
	SMO	37.78%	81.40%	59.09%

6.3.1 Step Detection Module

As the total number of steps is the final output of the step detection module, it is expected that the step count error will decrease if the INS would use a prediction module. Table 6.9 shows the step count error produced by the INS with and without a prediction module.

The straight and square routes both show that the INS without the prediction module performs better, with a five and nine step difference respectively. The INSs with a prediction module, on the other hand, achieved a lower error rate when it comes to the multi-activity routes. This suggests that an amount of false negatives had to be made in exchange for versatility, but the benefits outweigh

Table 6.9: The step count error produced by each model.

Test	Model Type	Actual No. of Steps	Estimated No. of Steps	Step Count Error
Straight Route	without	88	91	3.41%
	J48	83	91	9.64%
	SMO	83	91	9.64%
Multi-Activity Straight Route	without	234	110	52.99%
	J48	135	110	18.52%
	SMO	135	110	18.52%
Square Route	without	188	181	3.72%
	J48	188	176	6.38%
	SMO	188	180	4.26%
Multi-Activity Square Route	without	296	193	34.80%
	J48	233	193	17.17%
	SMO	233	193	17.17%

the disadvantages. INSs with prediction modules are more adaptable in terms of allowing the subject to perform negative pedestrian locomotion movements.

Figures 6.5 to 6.8 show a visualization of the actual number of steps against the estimated number of steps per test. The close precision of the estimates in the straight and square routes are apparent in the graphs.

Though there are portions in the straight and square route tests where the INS without a prediction module are more accurate, Figures 6.5 to 6.8 suggest that the J48 model is the best of option of the three.

Another test was done to evaluate the step detection module based on just the number of steps it can correctly detect. The route, as depicted in Figure 6.9, involves the subject to 1) move 10 steps in a natural pace, 2) stand for 5 seconds, 3) move 10 steps in a natural pace, and 4) walk-in-place for 5 seconds.

The J48 and SMO models across the eight different window sizes were evaluated based on each INS's estimated number of steps. Table 6.10 shows that the models that use 64-, 90-, and 100-sample window sizes attained the lowest step count errors, and J48 models generally perform better.

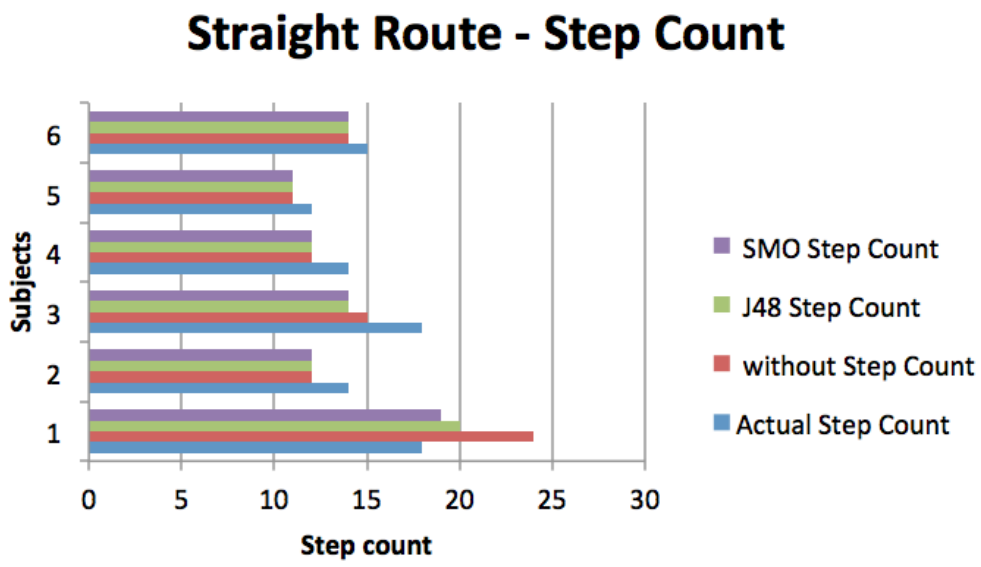

Figure 6.5: The graph above shows the real step count compared to those detected by INSs with and without the prediction modules for the Straight Route Test.

6.3.2 Stride Length Estimation Module

The total traversed length would also be analyzed as it is the final output of the stride length estimation module. The length error of INSs with and without a prediction module are presented in Table 6.11.

Like the results of the step detection module, the error is smaller based on the kind of test an INS undergoes. The INSs without a prediction module performed better on the purely positive pedestrian locomotion activities, while INSs with a prediction module is more suitable for multi-activity tests. But the error difference of the straight and square route tests are acceptable compared to the error difference in the other two tests, making it a tolerable trade for the flexibility the prediction module offers.

The actual traversed lengths of each subject is compared to the estimated of the INSs with and without a prediction module in Figures 6.10 to 6.13. The figure shows the precision of the length estimates in the straight and square route tests, while a large variance starts to appear with the multi-activity tests. In agreement with the figures shown in the Step Detection Module section, these figures also indicates that the J48 model shows a clear advantage in minimizing the total length error.

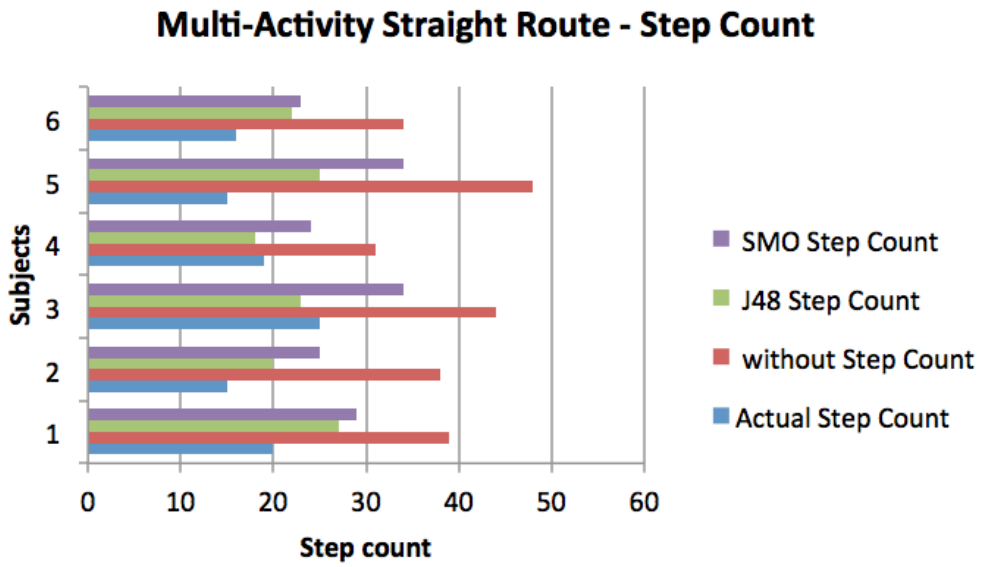

Figure 6.6: The graph above shows the real step count compared to those detected by INSs with and without the prediction modules for the Multi-Activity Straight Route Test.

6.3.3 Mapping Module

The final output of an INS is the route produced by the Mapping Module, and it shows a visualization of where a user has traversed. In this section, the models that have a 100 window size were used.

Figure 6.14 shows the resulting routes of the INSs in one subject's Square Route test data. The square route in black shows the actual route taken by the user. The INSs with the J48 and SMO models constructed the same route, so both routes are represented by the yellow path. In this figure, it is apparent that the INSs with the prediction module was able to estimate the actual route well, but failed to complete the last two meters in the right direction.

This test faired well because the angles are perpendicular. Since the mapping module fixes the orientation of the phone to its nearest secondary direction, the sharp perpendicular angles were rendered well.

Figure 6.15 displays the actual and predicted routes of a user walking along Gokongwei Building's 4th floor main hallway. The route in black shows the actual route taken by the user, and spans 65.2 meters. The red route represents the path

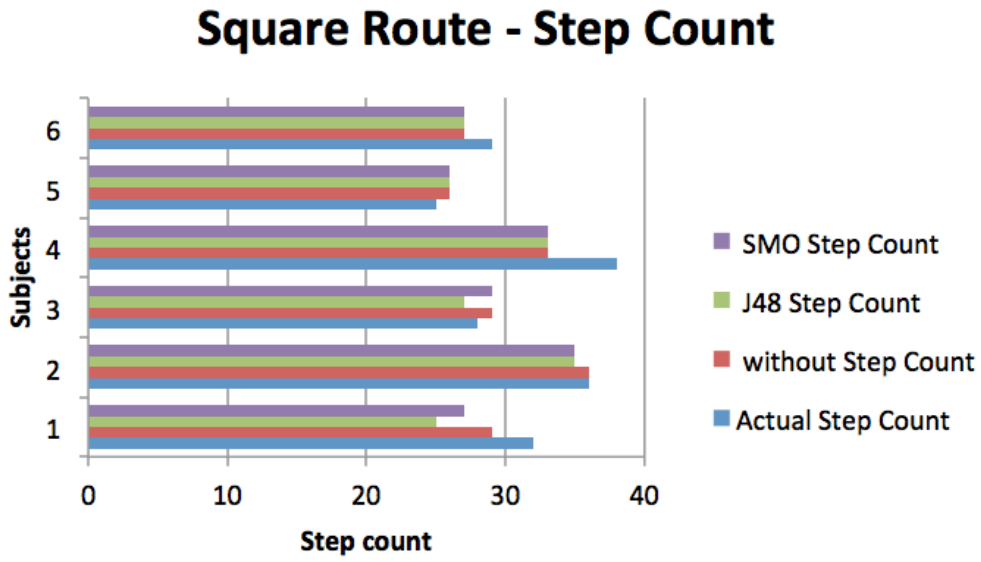

Figure 6.7: The graph above shows the real step count compared to those detected by INSs with and without the prediction modules for the Square Route Test.

estimated by the INS without the prediction module and the INS with the SMO model, while the green route represents the path estimated by the INS with the J48 model. Though the angles were clearly translated incorrectly, the estimated lengths were fairly precise. The green route is equivalent to 64.41m, while the red route is 74.28m long. The estimated routes were flawed mainly because the detected orientations were faulty.

A final test was done to check the INS's ability to map big routes. The result shown in Figure 6.16 is the route taken in Ayala Triangle Park, and is a combination of natural positive and negative pedestrian locomotion activities. The black route represents the actual route taken, the red route portrays the estimated path of the INS without a module, and the blue route corresponds to the estimated path of the INS with the J48 prediction model.

Though the path didn't fit well to the actual route, the lengths of each turn were depicted quite well. As the park route was shaped with angles that do not directly correspond to any of the secondary directions, the angles were translated incorrectly.

This test also showed the difference between the INS with and without the prediction module, with the latter overestimating the route than the former. The

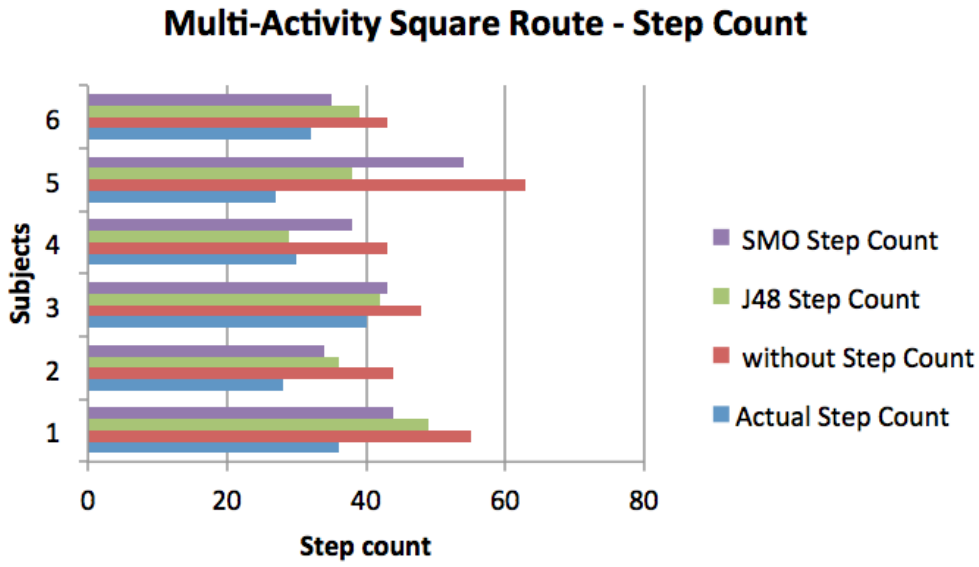

Figure 6.8: The graph above shows the real step count compared to those detected by INSs with and without the prediction modules for the Multi-Activity Square Route Test.

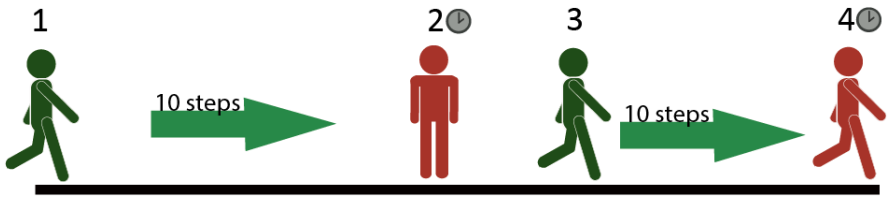

Figure 6.9: The user must 1) move 10 paces, 2) stand for 5 seconds, 3) move 10 paces, and 4) walk-in-place for 5 seconds in this test.

path estimated by the INS without the module was also characterized with more jitters, each of which adds 2-3 meters to the total traversed length.

Table 6.10: The performance of J48 and SMO models in the Step Detection Module Test.

Window Size - Overlap Size	Model Type	Actual Steps	Estimated Steps	Step Count Error
64-32	without	120	168	40.00%
	J48	120	118	1.67%
	SMO	120	129	7.50%
70-35	without	120	169	40.83%
	J48	120	112	6.67%
	SMO	120	41	65.83%
80-40	without	120	166	38.33%
	J48	120	105	12.50%
	SMO	120	25	79.17%
90-45	without	120	165	37.50%
	J48	120	112	6.67%
	SMO	120	112	6.67%
100-50	without	120	165	37.50%
	J48	120	130	8.33%
	SMO	120	133	10.83%
128-64	without	120	160	33.33%
	J48	120	116	3.33%
	SMO	120	34	71.67%
200-100	without	120	155	29.17%
	J48	120	96	20.00%
	SMO	120	7	94.17%
256-128	without	120	142	18.33%
	J48	120	78	35.00%
	SMO	120	17	85.83%

Table 6.11: The traversed length error produced by each model.

Test	Model Type	Actual Length	Estimated Length	Length Error
Straight Route	without	60	57.53	4.12%
	J48	60	54.19	9.68%
	SMO	60	53.51	10.81%
Multi-Activity Straight Route	without	60	154.24	157.07%
	J48	60	88.22	47.04%
	SMO	60	110.51	84.19%
Square Route	without	120	117.98	1.69%
	J48	120	114.70	4.41%
	SMO	120	117.29	2.26%
Multi-Activity Square Route	without	120	193.67	61.39%
	J48	120	151.97	26.64%
	SMO	120	161.65	34.71%

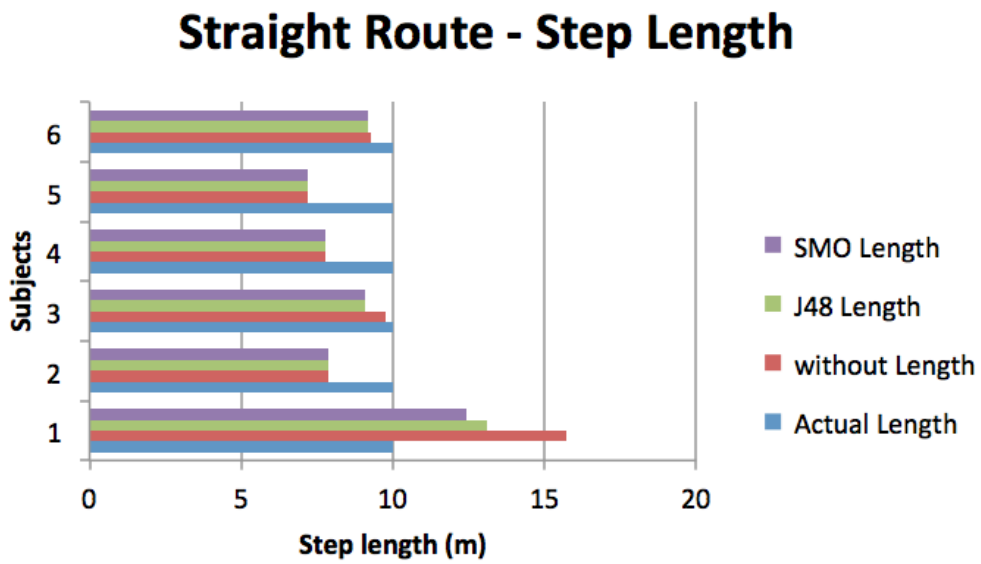

Figure 6.10: The graph above shows the real traversed length compared to those estimated by INSs with and without the prediction modules for the Straight Route Test.

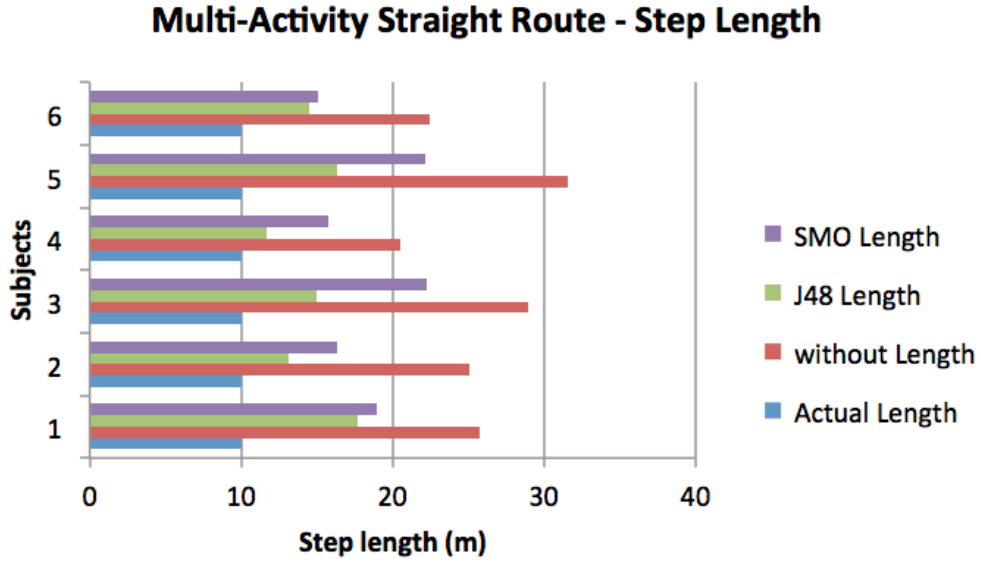

Figure 6.11: The graph above shows the real traversed length compared to those estimated by INSs with and without the prediction modules for the Multi-Activity Straight Route Test.

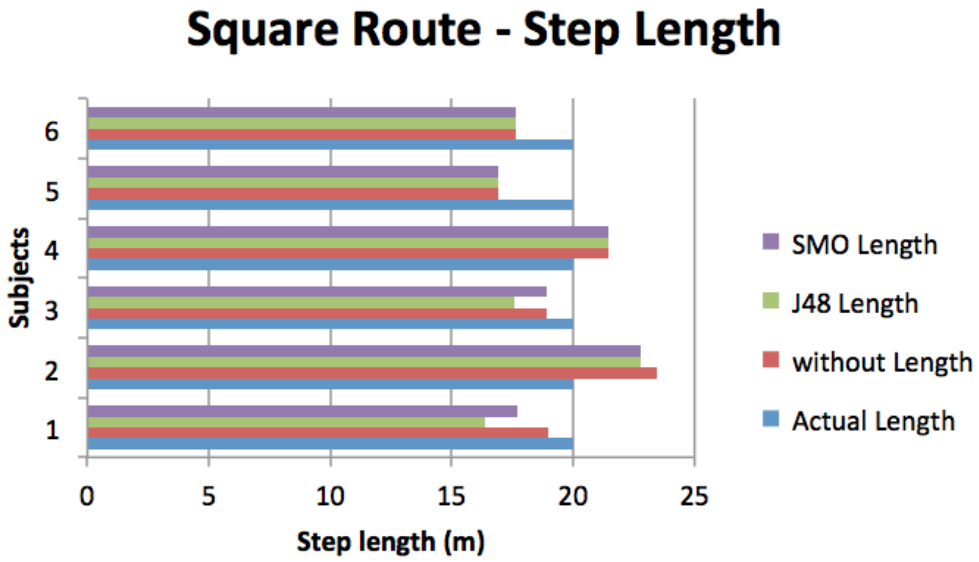

Figure 6.12: The graph above shows the real traversed length compared to those estimated by INSs with and without the prediction modules for the Square Route Test.

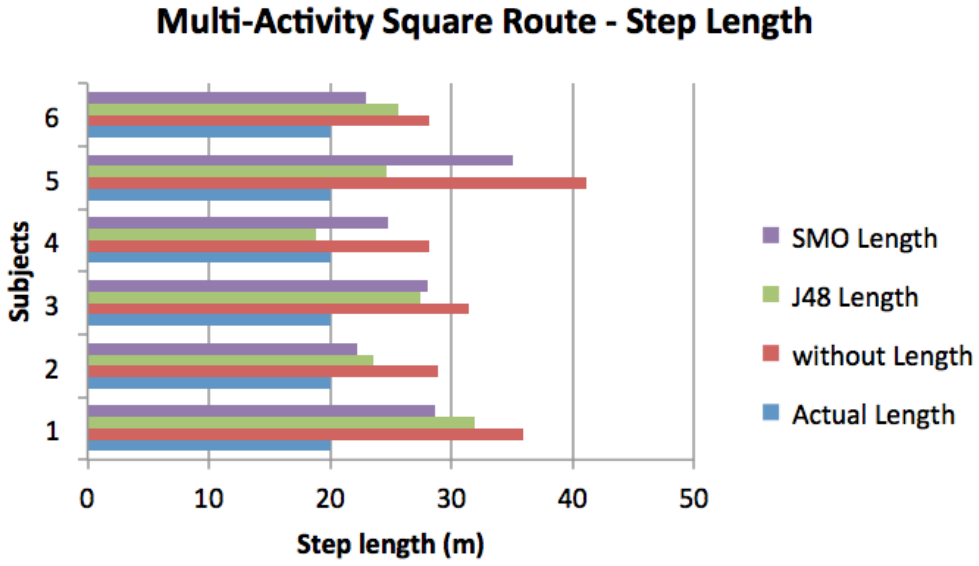

Figure 6.13: The graph above shows the real traversed length compared to those estimated by INSs with and without the prediction modules for the Multi-Activity Square Route Test.

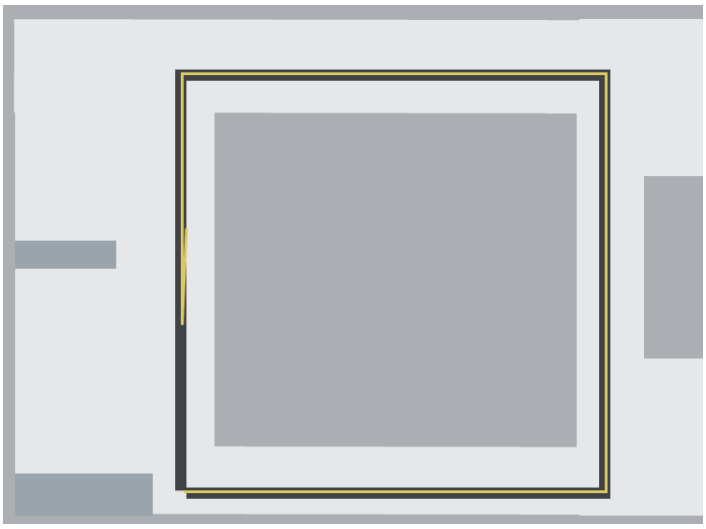

Figure 6.14: The figure above shows the actual route traversed by the user in black, and the route predicted by the INSs in yellow.

Figure 6.15: The black route shows the actual route taken by the user, while the red and blue paths are the routes estimated by the INSs.

Figure 6.16: The route in black is the actual route traversed by the user, and the routes in red and blue are the routes predicted by the INS without a module, and the INS with the J48 prediction model.

7 Conclusion and Recommendation

This research was able to present that a J48 and SMO pedestrian locomotion module can increase the over-all performance of an INS. The step detection and stride length estimation module also benefited from the prediction model especially with experiments that have negative pedestrian locomotion acitivities.

In the four tests that were conducted in this research to evaluate the INS, the models with a 100 sample window proved to be the best among all the models. The J48 and SMO models that were generated with this window size performed well in its 10-fold cross-validation evaluation, they have a consistent performance across all INS tests, and their effect over the other modules have been generally advantageous for the whole INS.

In conclusion, the results have shown that adding a pedestrian locomotion model allows an INS to be more versatile. An INS with a prediction module can handle negative pedestrian locomotion activity, while a normal INS will require users to walk continuously and maintain a low sensor activity to prohibit a negative pedestrian locomotion activity to be falsely considered a step. And as negative pedestrian locomotion activities are inevitable in real scenarios, a prediction module presents an adequate solution to this INS problem.

Further research can develop a better model by adding more positive and negative activities, and also test out other features that are also discriminative. As this research cannot handle data of a person running or moving at a different pace, it would be useful to add that activity in subsequent studies.

Limitations of the phone's orientation can also be a topic of research in the future. The ability of the INS to correctly identify a person moving the phone from its position and properly discount those data would be a useful characteristic for a mobile app.

Evaluating the model in other more realistic scenarios is also another possible path to study on. Tests that will allow people to move freely around a space will gauge the ability and limitations of the model, and would possibly lead to robust models.

8 Acknowledgement

This research is made possible with funding from the Philippine government. The researchers would like to thank the Department of Science and Technology's Engineering Research and Development for Technology (DOST-ERDT) program for its incalculable support for this study.

A Appendix A - Discriminative Ability of the Features

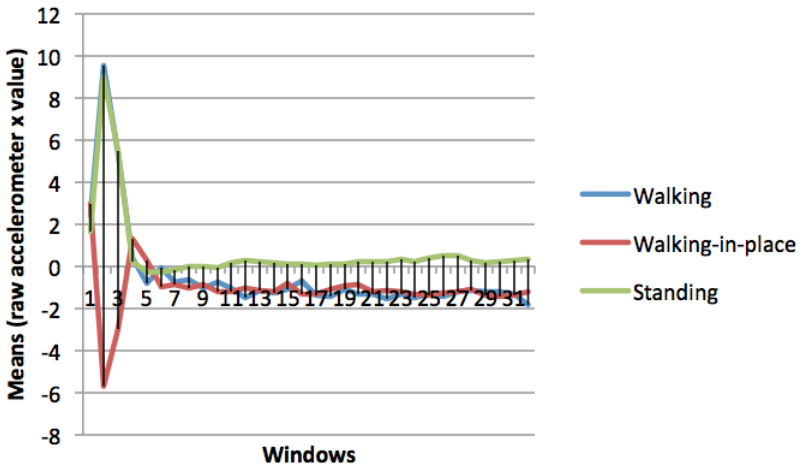

Figure A.1: An example showing the ability of the means of the raw accelerometer x-axis values to discriminate between negative and positive pedestrian locomotion activities.

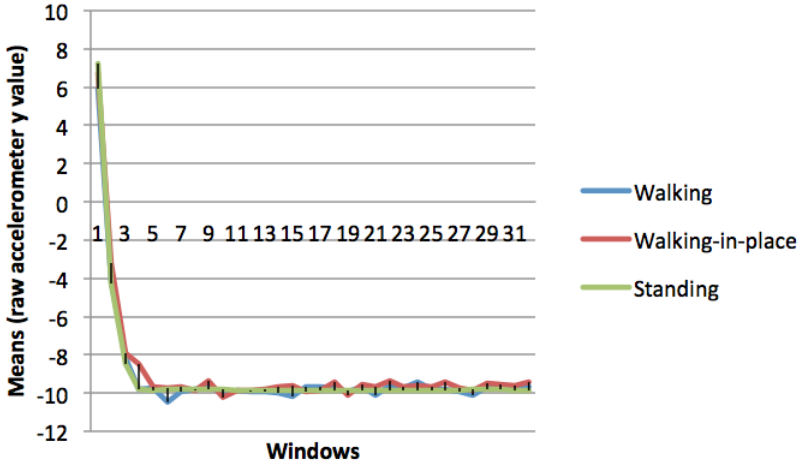

Figure A.2: An example showing the ability of the means of the raw accelerometer y-axis values to discriminate between negative and positive pedestrian locomotion activities.

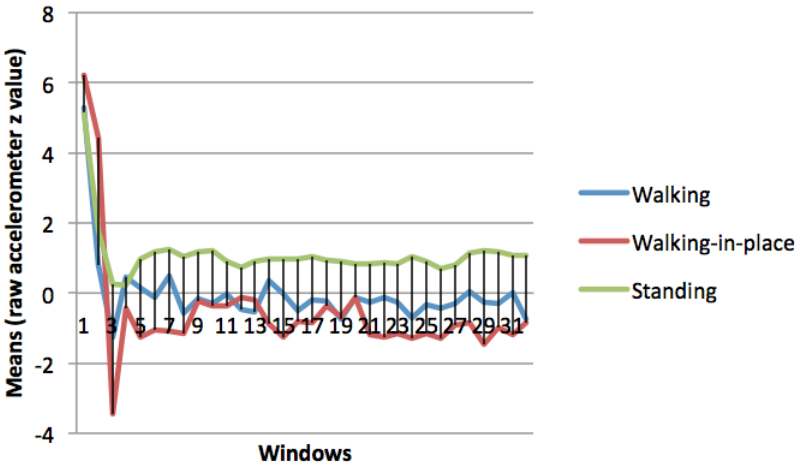

Figure A.3: An example showing the ability of the means of the raw accelerometer z-axis values to discriminate between negative and positive pedestrian locomotion activities.

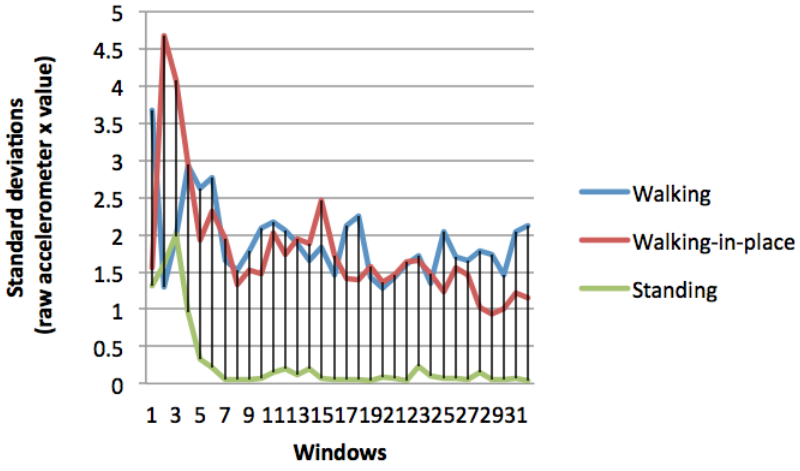

Figure A.4: An example showing the ability of the standard deviations of the raw accelerometer x-axis values to discriminate between negative and positive pedestrian locomotion activities.

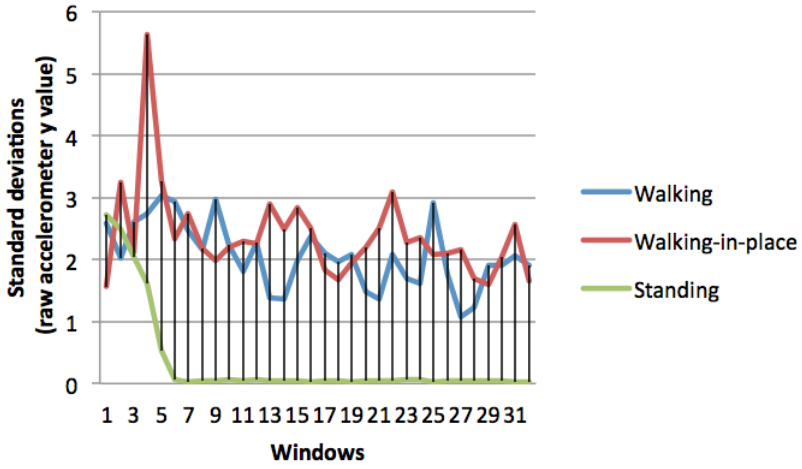

Figure A.5: An example showing the ability of the standard deviations of the raw accelerometer y-axis values to discriminate between negative and positive pedestrian locomotion activities.

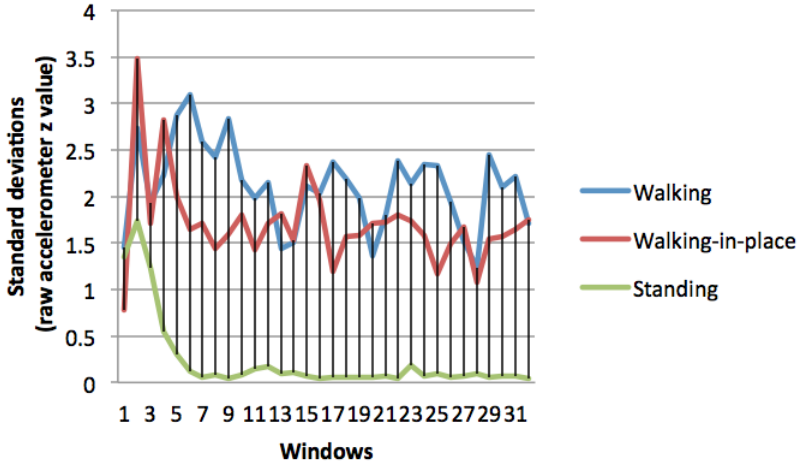

Figure A.6: An example showing the ability of the standard deviations of the raw accelerometer z-axis values to discriminate between negative and positive pedestrian locomotion activities.

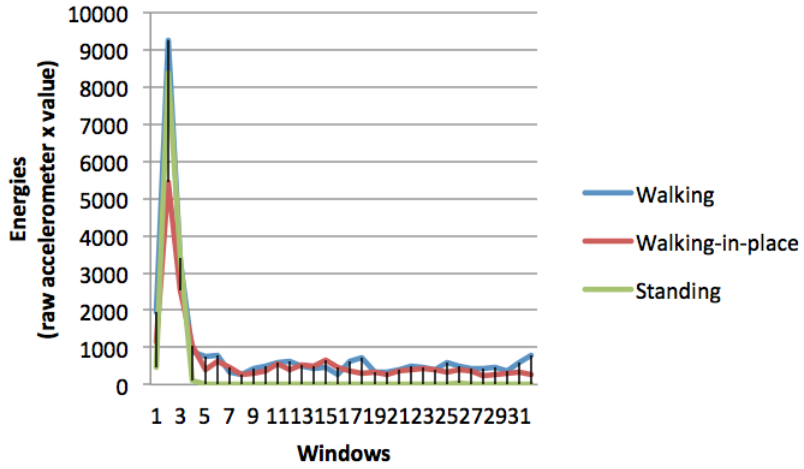

Figure A.7: An example showing the ability of the energies of the raw accelerometer x-axis values to discriminate between negative and positive pedestrian locomotion activities.

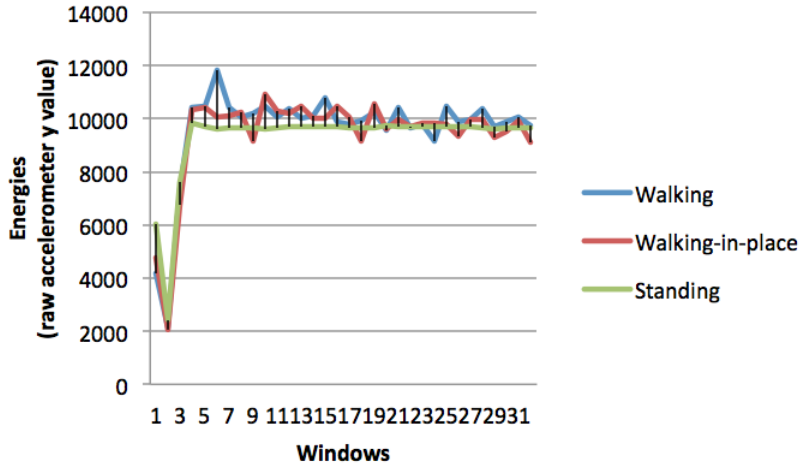

Figure A.8: An example showing the ability of the energies of the raw accelerometer y-axis values to discriminate between negative and positive pedestrian locomotion activities.

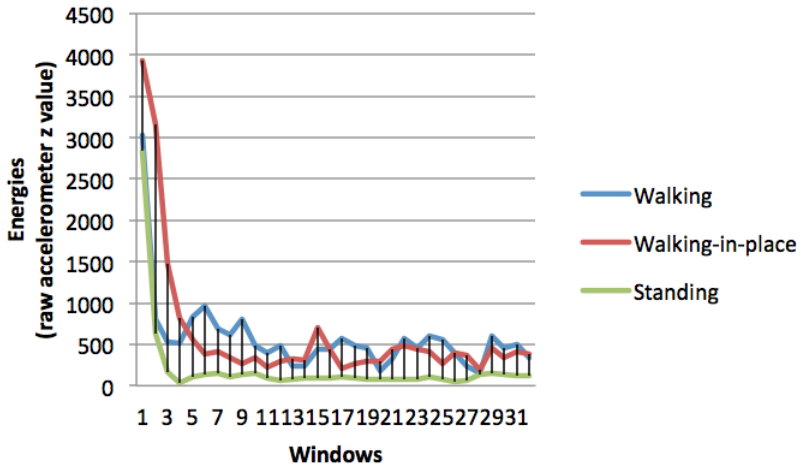

Figure A.9: An example showing the ability of the energies of the raw accelerometer z-axis values to discriminate between negative and positive pedestrian locomotion activities.

B Appendix B - Selected Attributes Used in the Models

Table B.1: The selected attributes for the J48 and SMO models that use the 64-sample window size.

J48	SMO
Accx_stddev	Accx_stddev
Accy_stddev	Accx_energy
Accy_energy	Accy_mean
Accz_stddev	Accy_stddev
Accz_energy	Accy_energy
Gyrox_mean	Accy_fdom
Gyrox_stddev	Accz_energy
Gyrox_energy	Gyrox_energy
Gyroy_stddev	Gyrox_fdom
Gyroy_energy	Gyroy_energy
Gyroz_stddev	Gyroz_energy
Gyroz_energy	Gyromag_fdom

Table B.2: The selected attributes for the J48 and SMO models that use the 70-sample window size.

J48	SMO
Accx_stddev	Accx_stddev
Accy_stddev	Accx_energy
Accy_energy	Accy_stddev
Accz_stddev	Accy_energy
Accz_energy	Accz_mean
Gyrox_mean	Accz_stddev
Gyrox_stddev	Accz_energy
Gyrox_energy	Gyrox_energy
Gyroy_stddev	Gyroy_energy
Gyroy_energy	Gyroy_fdom
Gyroz_stddev	Gyroz_mean
Gyroz_energy	Gyroz_energy

Table B.3: The selected attributes for the J48 and SMO models that use the 80-sample window size.

J48	SMO
Accx_stddev	Accx_stddev
Accx_energy	Accx_energy
Accy_stddev	Accy_stddev
Accy_energy	Accy_energy
Accz_stddev	Accz_stddev
Accz_energy	Accz_energy
Gyrox_energy	Gyrox_energy
Gyroy_energy	Gyroy_energy
Gyroy_fdom	Gyroy_fdom
Gyroz_mean	Gyroz_mean
Gyroz_energy	Gyroz_energy

Table B.4: The selected attributes for the J48 and SMO models that use the 90-sample window size.

J48	SMO
Accx_stddev	Accx_stddev
Accy_stddev	Accy_stddev
Accy_energy	Accy_energy
Accz_stddev	Accz_mean
Accz_energy	Accz_stddev
Gyrox_stddev	Accz_energy
Gyrox_energy	Gyrox_energy
Gyroy_stddev	Gyroy_energy
Gyroy_energy	Gyroy_fdom
Gyroz_stddev	Gyroz_mean
Gyroz_energy	Gyroz_energy

Table B.5: The selected attributes for the J48 and SMO models that use the 100-sample window size.

J48	SMO
Accx_stddev	Accx_stddev
Accy_stddev	Accy_stddev
Accy_energy	Accy_energy
Accz_stddev	Accz_mean
Accz_energy	Accz_stddev
Gyrox_stddev	Accz_energy
Gyrox_energy	Gyrox_energy
Gyroy_stddev	Gyrox_fdom
Gyroy_energy	Gyroy_mean
Gyroz_stddev	Gyroz_mean
Gyroz_energy	Gyroz_stddev
	Gyroz_energy

Table B.6: The selected attributes for the J48 and SMO models that use the 128-sample window size.

J48	SMO
Accx_stddev	Accx_stddev
Accy_stddev	Accy_stddev
Accy_energy	Accy_energy
Accz_stddev	Accz_mean
Accz_energy	Accz_stddev
Gyrox_stddev	Gyrox_energy
Gyrox_energy	Gyroy_stddev
Gyroy_stddev	Gyroz_mean
Gyroy_energy	Gyroz_energy
Gyroz_stddev	
Gyroz_energy	

Table B.7: The selected attributes for the J48 and SMO models that use the 200-sample window size.

J48	SMO
Accx_stddev	Accx_stddev
Accy_stddev	Accx_energy
Accy_energy	Accy_stddev
Accz_stddev	Accy_energy
Accz_energy	Accz_stddev
Gyrox_stddev	Accz_energy
Gyrox_energy	Gyrox_energy
Gyroy_stddev	Gyroy_stddev
Gyroy_energy	Gyroy_fdom
Gyroz_stddev	Gyroz_mean
Gyroz_energy	Gyroz_energy

Table B.8: The selected attributes for the J48 and SMO models that use the 256-sample window size.

J48	SMO
Accx_stddev	Accx_stddev
Accy_stddev	Accx_energy
Accy_energy	Accy_mean
Accz_stddev	Accy_stddev
Accz_energy	Accy_energy
Gyrox_stddev	Accz_stddev
Gyrox_energy	Accz_energy
Gyroy_stddev	Gyrox_stddev
Gyroy_energy	Gyrox_energy
Gyroz_mean	Gyroy_stddev
Gyroz_stddev	Gyroy_fdom
Gyroz_energy	Gyroz_mean
Gyroz_fdom	Gyroz_energy

C Appendix C - The Effect of Window Sizes in Model Performance

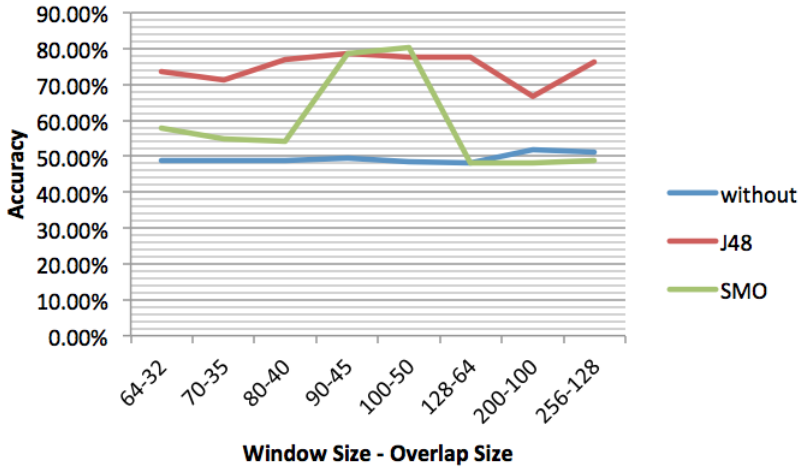

Figure C.1: The performances of the J48 and SMO models vary as the window size changes.

References

Aaron Burg, B. S. M. W., Azeem Meruani. (n.d.). *Mems gyroscopes and their applications: A study of the advancements in the form, function, and use of mems gyroscopes.* Lecture Notes.

Android, G. (2013). *Sensors overview.* Available from `http://developer.android.com/guide/topics/sensors/sensors_overview.html`

Anguita, D., Alessandro, G., Oneto, L., Parra, X., & Reyes-Ortiz, J. (2012). Human activity recognition on smartphones using a multiclass hardware-friendly support vector machine. In *Iwaal* (p. 216-223).

Bryan, G. H. (n.d.). On the beats in the vibrations of a revolving cylinder or bell. In *Proc. of cambridge phil. soc.*

Cho, D.-K., Mun, M., Lee, U., Kaiser, W. J., & Gerla, M. (2010). Autogait: A mobile platform that accurately estimates the distance walked. In *Percom* (p. 116-124). IEEE Computer Society. Available from `http://dblp.uni-trier.de/db/conf/percom/percom2010.htmlChoMLKG10`

Cho, S. Y., & Park, C. G. (2006). Mems based pedestrian navigation system. In *The journal of navigation* (pp. 135–163). Seoul: The Royal Institute of Navigation.

Ermes, M., Parkka, J., Mantyjarvi, J., & Korhonen, I. (2008). Detection of daily activities and sports with wearable sensors in controlled and uncontrolled conditions. *Trans. Info. Tech. Biomed.*, *12*(1), 20–26.

Gyllensten, I. C., & Bonomi, A. G. (2011). Identifying types of physical activity with a single accelerometer: Evaluating laboratory-trained algorithms in daily life. *IEEE Trans. Biomed. Engineering*, *58*(9), 2656-2663.

Inc., A. (2012, August). *Mac notebooks: About the sudden motion sensor.* Available from `http://support.apple.com/kb/ht1935`

Kothari, N., Kannan, B., Glasgwow, E. D., & Dias, M. B. (2012). Robust indoor localization on a commercial smart phone. *Procedia CS*, *10*, 1114-1120.

Lee, S.-W., & Mase, K. (2001). Recognition of walking behaviors for pedestrian navigation. In *Proceedings of the 2001 ieee international conference on control applications* (pp. 1152–1155).

Li, F., Zhao, C., Ding, G., Gong, J., Liu, C., & Zhao, F. (2012). A reliable and accurate indoor localization method using phone inertial sensors. In *Proceedings of the 2012 acm conference on ubiquitous computing* (pp. 421–430). New York, NY, USA: ACM. Available from `http://doi.acm.org/10.1145/2370216.2370280`

Libby, R. (2008, June). *A simple method for reliable footstep detection in embedded sensor platforms.* (normal checking with low pass filter)

LLC, D. E. (n.d.). *A beginner's guide to accelerometers.* Available from `http://www.dimensionengineering.com/info/accelerometers`

Martin, J. D., Krosche, J., & Boll, S. (n.d.). Dynamic gps-position correction for mobile pedestrian navigation and orientation. In *Proceedings of the 3rd workshop on positioning, navigation and communication.*

Mathie, M. (2003). *Monitoring and interpreting human movement patterns using a triaxial accelerometer*. University of New South Wales. Available from `http://books.google.com.ph/books?id=f87DtgAACAAJ`

Melissa Selik, A. B., Richard Baranuik. (2004, August). *Signal energy vs signal power*. Online.

Moell, V., & Horntvedt, A. (2012). *Positioning for mobile phones using wlan and accelerometer data*. Unpublished master's thesis, Lunds Universitet.

Nam, Y. (2011). Map-based indoor people localization using an inertial measurement unit. *J. Inf. Sci. Eng.*, *27*(4), 1233-1248.

Nanocomputers and swarm intelligence. (2008). London: John Wiley and Sons.

Parnandi, A., Le, K., Vaghela, P., Kolli, A., Dantu, K., Poduri, S., et al. (2009?). Coarse in-building localization with smartphones.

Platt, J. C. (1999). Advances in kernel methods. In B. Schölkopf, C. J. C. Burges, & A. J. Smola (Eds.), (pp. 185–208). Cambridge, MA, USA: MIT Press. Available from `http://dl.acm.org/citation.cfm?id=299094.299105`

Quinlan, J. R. (1993). *C4.5: programs for machine learning*. San Francisco, CA, USA: Morgan Kaufmann Publishers Inc.

Renaudin, V., Susi, M., & Lachapelle, G. (2012). Step length estimation using handheld inertial sensors. *Sensors*, *12*(7), 8507–8525. Available from `http://www.mdpi.com/1424-8220/12/7/8507`

Ronald E. Walpole, S. L. M. K. Y., Raymond H. Myers. (2010). Scientists and engineers: Guide to probability and statistics. In (chap. 1). Pearson Education South Asia Pte. Ltd.

Shala, U., & Rodriguez, A. (2011). *Indoor positioning using sensor-fusion in android devices*. Unpublished master's thesis, Kristianstad University, School of Health and Society.

STMicroelectronics. (n.d.). L3g4200d mems motion sensor: ultra-stable three-axis digital output gyroscope [Computer software manual].

Susi, M., Renaudin, V., & Lachapelle, G. (2013). Motion mode recognition and step detection algorithms for mobile phone users. *Sensors*, *13*(2), 1539–1562. Available from `http://www.mdpi.com/1424-8220/13/2/1539`

Tan, S. (2008). Linear systems. In (chap. 8). University of Auckland.

Thanh, T. N., Makihara, Y., Nagahara, H., Mukaigawa, Y., & Yagi, Y. (2012a). Inertial-sensor-based walking action recognition using robust step detection and inter-class relationships. In *Icpr* (p. 3811-3814).

Thanh, T. N., Makihara, Y., Nagahara, H., Mukaigawa, Y., & Yagi, Y. (2012b). Performance evaluation of gait recognition using the largest inertial sensor-based gait database. In *Icb* (p. 360-366).

Walpole, R. E. (2009). Introduction to statistics. In (chap. 2). Pearson Education

South Asia Pte Ltd.

Won Kim, J., Jin Jang, H., Hwang, D. H., & Park, C. (2004). A step, stride and heading determination for the pedestrian navigation system. *Journal of Global Positioning System*. (shoe embedded)

Ying, H., Silex, C., Schnitzer, A., Leonhardt, S., & Schiek, M. (2007). Automatic step detection in the accelerometer signal. In S. Leonhardt, T. Falck, & P. M√§h√∂nen (Eds.), *4th international workshop on wearable and implantable body sensor networks (bsn 2007)* (Vol. 13, p. 80-85). Springer Berlin Heidelberg. Available from http://dx.doi.org/10.1007/978-3-540-70994-7_14